



Editorial

Three-dimensional ultrasound imaging of the fetal skull and face

B. TUTSCHEK^{1,2*}, H.-G. K. BLAAS³, J. ABRAMOWICZ⁴, K. BABA⁵, J. DENG⁶, W. LEE⁷,
E. MERZ⁸, L. PLATT⁹, D. PRETORIUS¹⁰, I. E. TIMOR-TRITSCH¹¹ and L. GINDES¹²,
for the ISUOG 3D Special Interest Group

¹Prenatal Zurich, Zürich, Switzerland; ²Medical Faculty, Heinrich Heine University, Düsseldorf, Germany; ³Department of Laboratory Medicine, Children's and Women's Health, Norwegian University of Science and Technology, National Center for Fetal Medicine, St Olavs Hospital, Trondheim, Norway; ⁴Department of Obstetrics and Gynecology, University of Chicago, Chicago, IL, USA; ⁵Saitama Medical Center, Saitama Medical University, Kawagoe, Japan; ⁶University College London, London, UK; ⁷Baylor College of Medicine, Obstetrics & Gynecology, Houston, TX, USA; ⁸Krankenhaus Nordwest - Centre for Prenatal Diagnosis and Therapy, Frankfurt, Germany; ⁹Department of Obstetrics and Gynecology, David Geffen School of Medicine at UCLA, Los Angeles, CA, USA; ¹⁰Department of Radiology, University of California San Diego, CA, USA; ¹¹Department of Obstetrics and Gynecology, NYU School of Medicine, New York, NY, USA; ¹²Department of Obstetrics and Gynecology, Wolfson Medical Center, and Sackler School of Medicine, Tel-Aviv University, Tel Aviv, Israel

*Correspondence. (e-mail: tutschek@me.com)

KEYWORDS: 3D ultrasound; face; prenatal diagnosis; skull

Short title: *3D-US of fetal skull and face*

Introduction

Assessment of the fetal skull and face is an integral part of the sonographic fetal anatomy examination. Ultrasound (US) is an accurate tool with which to detect craniofacial malformations prenatally¹. In a routine scan, the skull dimensions are measured and the head's shape and integrity are assessed subjectively. The brain structures are documented in two standard axial views, depicting the bones of the calvarium. The face is imaged to show eyes, profile and lips², while also demonstrating important osseous landmarks.

Standard views are routinely obtained using two-dimensional (2D) imaging, but volume (three-dimensional (3D)) US is an important adjunct for assessment of the fetal skull and face³. The individual cranial bones, sutures and fontanels are more difficult to visualize using 2D imaging, because the cranial bones represent curvilinear plates, which are difficult or impossible to depict in a single cross-section, but well-suited to 3D-US⁴⁻⁶. In this Editorial, we describe 3D imaging of the bony structures of the fetal head and face; assessment of the fetal brain is not part of this overview.

Development of facial and skull bones

The facial bones develop by enchondral ossification from a number of ossification centers. Their development has been studied with 3D-US, using frontal insonation⁷. The maxilla and mandible are among the first skull bones that become visible on US, at 9 postmenstrual weeks. Frontal bone ossification begins at 9 weeks bilaterally above the eyes and extends laterally and cranially to form the frontal bones. In the normal fetus, the nasal bones are present from 10 weeks bilaterally and are distinct from the maxilla. The frontal bones of both sides expand centrifugally and approach each other in the midline, where they are separated by the metopic suture. The metopic suture narrows in the third trimester from the glabella to the top of the head, with progressive reduction of the width of the anterior fontanel (Figure S1).

The sutures and fontanels separate the individual external bones of the skull (Figure S2). The most easily recognized sutures are the metopic (frontal), coronal, sagittal and lambdoid sutures⁴. The sagittal, coronal and lambdoid sutures border the anterior and posterior fontanels. While these membranous areas of the skull are often exploited as acoustic windows into the fetal brain, particularly in later gestation, their osseous components can also be studied, because they can be affected by a variety of pathological conditions.

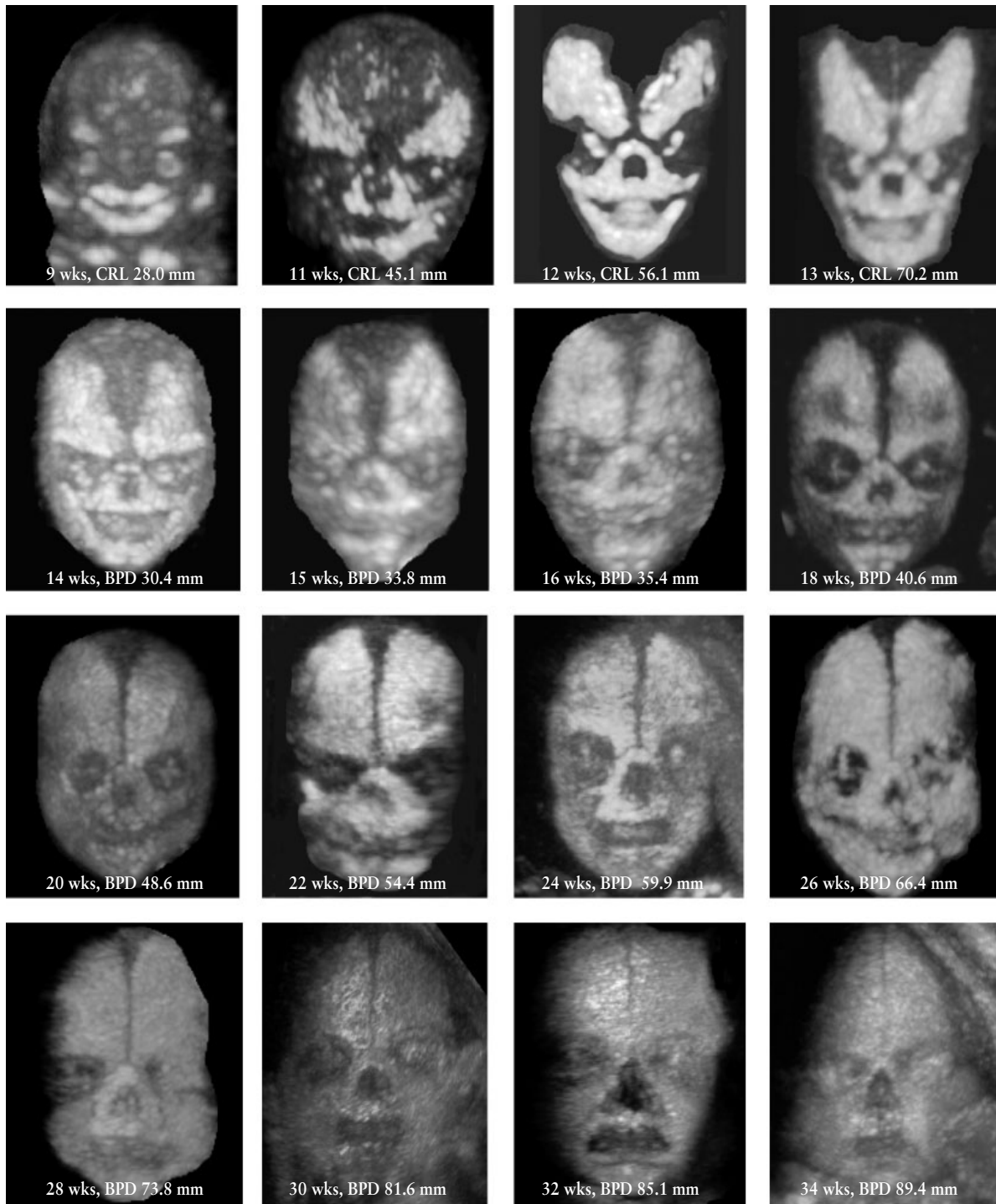


Figure S1 Normal development of fetal facial bones and sutures from 9 to 34 weeks (reproduced from Faro *et al.*⁷, with permission). The normal metopic suture between the two frontal bones closes from 16 to 32 weeks⁷.

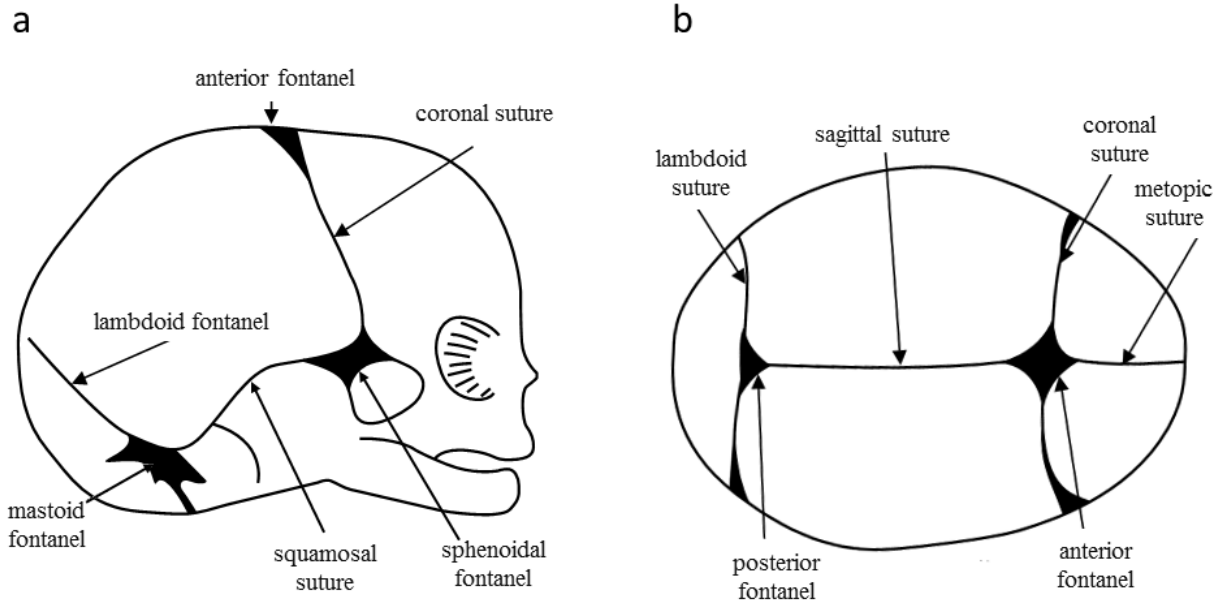


Figure S2 Schematic representation of normal cranial sutures and fontanels (modified from Delahaye *et al.*⁷¹, with permission): (a) lateral aspect; (b) seen from above, looking down on cranium.

Targeted volume acquisition, alignment and analysis

On B-mode imaging, normal cortical bone typically appears ‘bright’, or hyperechoic, as it has an acoustic impedance approximately six times greater than that of soft tissue⁸. Because the large cranial bones are curvilinear plates, they are often better displayed using 3D- than 2D-US⁴⁻⁶. Before acquiring a volume, 2D imaging must first be optimized for hyperechoic bone with regard to gain, focus and, possibly, harmonic imaging. Then, before the volume is acquired, the 3D settings for depth and width should be adjusted to include the whole volume of interest and as little other tissue as possible. Spatial resolution can be maximized using a slow sweep speed that is possible only in the presence of fetal quiescence. The US beam should be perpendicular to the bones of interest, mandating different insonation angles for different bones and sutures. A single insonation angle cannot show all bones and sutures in their entirety as refractive shadowing occurs at the curved edges (Figure S3). A videoclip showing acquisition and alignment of a volume of a normal mid-trimester fetal face is available at <http://sf.fetal.ch>.

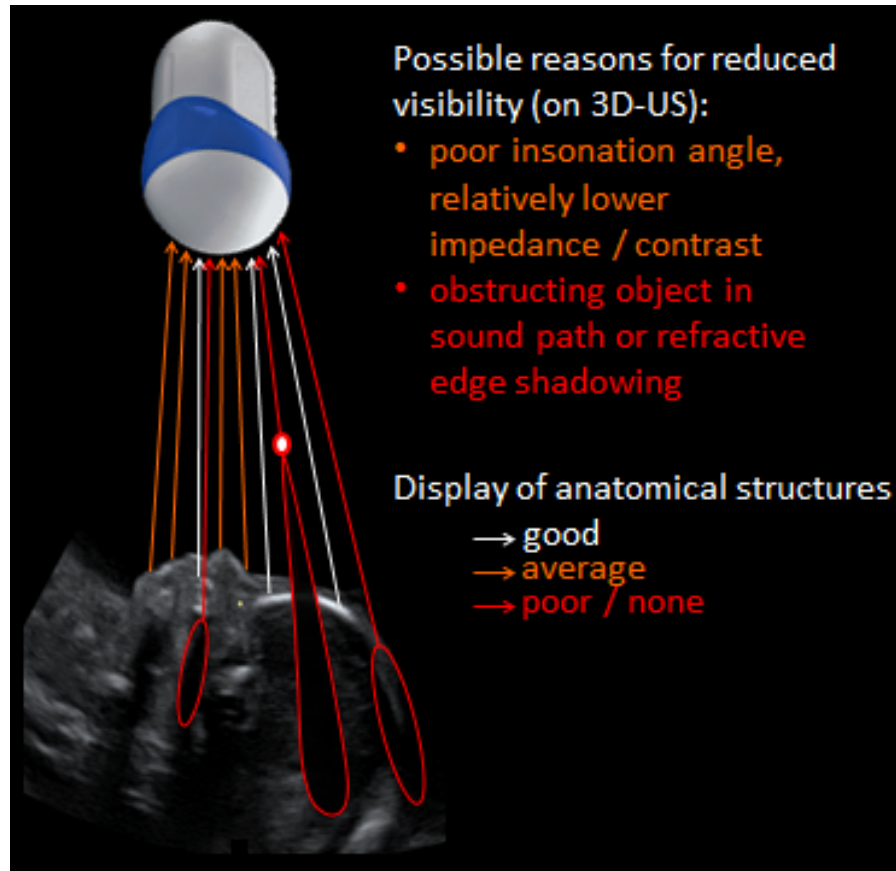


Figure S3 Possible reasons for reduced or lack of visibility of structures using two-dimensional and three-dimensional (3D) ultrasound (US). Note that internal bones in particular, such as the palate, are often affected by shadowing. Structures that are not insonated at or close to a right angle suffer most from reduced axial resolution.

3D-US volumes can be analyzed visually in two principal ways: by obtaining ('reformatting') cross-sections or by showing surface-rendered views. Cross-sections can be displayed either as a single plane or as two or three (usually orthogonal) planes together; in this Editorial we refer to the latter as 'multiplanar'. A display consisting of a number of parallel, equally spaced and sized cross-sections is also possible and is referred to as 'tomographic'. In cross-sectional display modes, volume contrast enhancement and curved planes can also be used. Surface-rendered views are spatially formatted displays of tissue interfaces of soft tissue (e.g. facial skin surface) or bone (e.g. skull bones) or a mixture of both.

Multiplanar imaging allows identification and spatial confirmation of any point contained in the volume by inspection of its position in the other two (usually) orthogonal planes of the multiplanar display. This is done by placing the reference dot (the intersection of the three planes) within the structure of interest, followed by inspection of this point in the other two planes. The final display can contain one plane which can be used, for example, to present an optimally aligned fetal profile (see Figure 2) or a multiplanar display. Figure S4 shows an example of a multiplanar display, with the reference dot, i.e. the intersection of the three planes, highlighted in red. In this volume display, in the axial plane, the location of the reference dot appears similar whether placed in the mandible or in the maxilla, but correlation of the reference dot in the three planes reveals the true anatomical position.

A variation of cross-sectional imaging involves placing a curved plane to display curved anatomical structures that do not lie in a straight plane, such as the palate (see Figure 5).

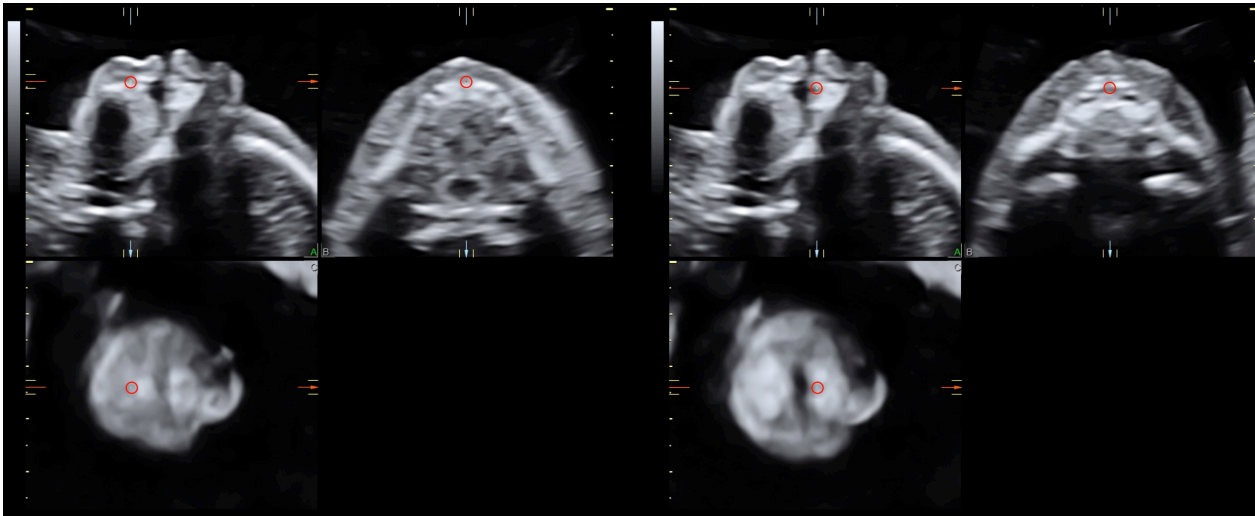


Figure S4 Confirmation of true anatomical relationships using multiplanar analysis: two multiplanar displays from the same volume of a normal fetal face. In (a), the reference dot (highlighted by red circle) is in the mandible. However, if only the axial plane is inspected, one might mistake the intact mandible for an intact maxilla. It is only when the reference dot's position is confirmed to be in the maxilla (b) that a cleft of the alveolar ridge can truly be excluded. Upper left images are sagittal, upper right images are axial and lower left images are coronal planes.

Tomographic imaging may provide detailed information that cannot be or is not easily obtained on real-time scanning⁹⁻¹². It can also be used for assessment of the fetal skull, for example for assessment of the bony components of the profile in suspected micrognathia or to confirm the continuity of the palate and the tooth buds (see Figures 2, S5, S6 and S14).

To obtain rendered views, displaying outer or inner surfaces, the so-called render box determines a volume of interest for the 3D/4D rendering algorithm. It defines the exclusive volume in which structures will be considered for spatial reconstruction (Figure 1). It also determines the direction of view towards the reconstructed structure. The render box can be adapted to encompass the entire anatomical structure of interest. The 'maximum intensity projection' algorithm is useful to display skeletal structures, such as the fetal skull¹³. Changing the postprocessing settings allows display of surface views for the skin and/or the bones from the same volume (Figure 1).

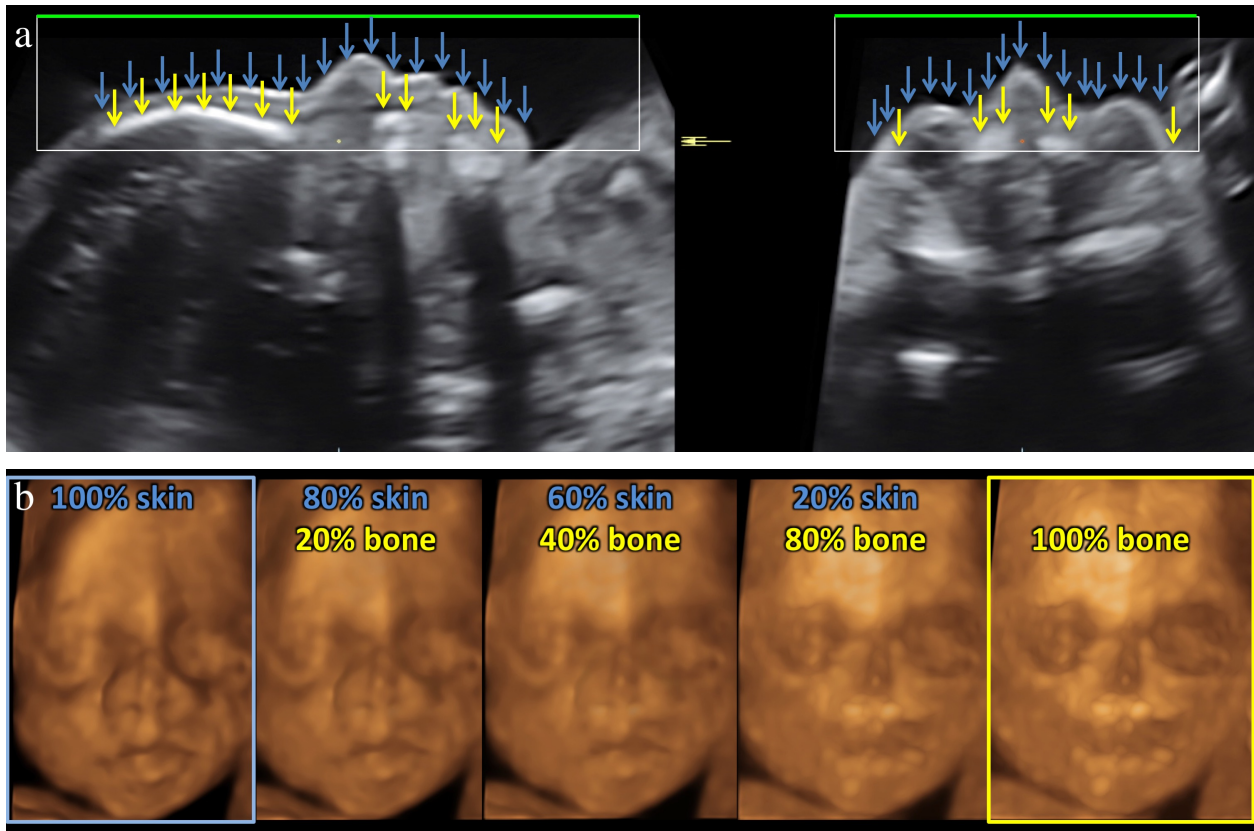


Figure 1 Optimized insonation of fetal face: surface display using render box. (a) Sagittal (left image) and axial (right image) views of face. Render box is operator-defined. Green line defines direction of rendering (not necessarily final direction from which object is eventually viewed). Blue and yellow arrows in (a) define soft tissues and bone elements, respectively, seen in display in (b). Ideally, the fetal face is insonated frontally, with at least a small amount of amniotic fluid between the face and other echogenic structures beneath the transducer, in particular bones of the extremities. (b) The same volume can be ‘rendered’ for either skin surface (‘100% skin’, far left) or bone surface (‘100% bone’, far right) or a variable mix of both. Note absence of ossification of both nasal bones in far right image in (b) in this fetus with trisomy 21.

Profile

Examination of the fetal profile can provide valuable information about malformations or genetic syndromes^{14,15}. The systematic 2D- and 3D-US assessment of normal and abnormal fetal facial anatomy and the profile has been described^{1,16}. 3D-US multiplanar display is an excellent tool for the fetal face and profile^{3,17-19}. A major benefit of 3D- over 2D-US is that the face and skull can be aligned accurately in standard anatomical planes, enabling objective assessment of facial symmetry or asymmetry in multiplanar and tomographic displays (Figures S5 and S6). An aligned volume can also be used for accurate quantitative measurements of bone sizes, relationships and angles. The precise midsagittal plane can never be known on 2D-US. Merz *et al.*²⁰ showed that a true profile is obtained with 2D-US in only 70% of patients and that presumed 2D profile images can be significantly oblique in 30% of patients. An example of how to acquire and align a fetal facial volume is shown at <http://sf.fetal.ch>.

The profile is best assessed subjectively and measured objectively when it is turned upright (Figures 2, S5 and S6). Line and angle can be applied to analyze the relationship between the anatomical landmarks. In a true midsagittal profile, three osseous landmarks can be used to describe basic facial parameters: (1) the nasion, the most anterior part at the intersection of the

frontal and nasal bones; and the most anterior points of (2) the maxilla and (3) the mandible²¹ (Figure 2). A normal face appears upright when the nasion and the anterior end of the mandible are aligned vertically.

The fetal facial profile line (FP)²² passes through the midpoint of the anterior border of the mandible and the nasion (green line in Figure 2). The frontal bone may recede behind the FP line ('negative FP') or extend frontally ('positive FP'). In normal fetuses, the FP line is at zero or mildly positive; it is negative in microcephalic and often in trisomy 18 fetuses; it is strongly positive if there is frontal bossing^{19,21,22}. The position of the FP line normally changes with increasing gestation, in part because, after 27 weeks, the forehead assumes a more rounded shape²².

The acute angle formed by the line from nasion to maxilla and the FP line is the maxilla-nasion-mandible (MNM) angle¹⁵ (Figure 2), which is 13.5° (median; 5th centile, 10.4°; 95th centile, 16.5°) in normal second- and third-trimester fetuses. In the normal fetal face, the relatively prominent jaws cause the typical concavity of the profile as opposed to the flatter adult profile¹⁵. The MNM angle is large in the presence of micrognathia, retrognathia or a combination of these, and is small in fetuses with trisomy 21²¹.



Figure S5 Volume alignment of frontally acquired normal fetal face (20 weeks). (a) Volume as acquired (frontal insonation, starting plane of volume scan oblique and parasagittal). (b) Same volume aligned anatomically and with profile rotated upright.

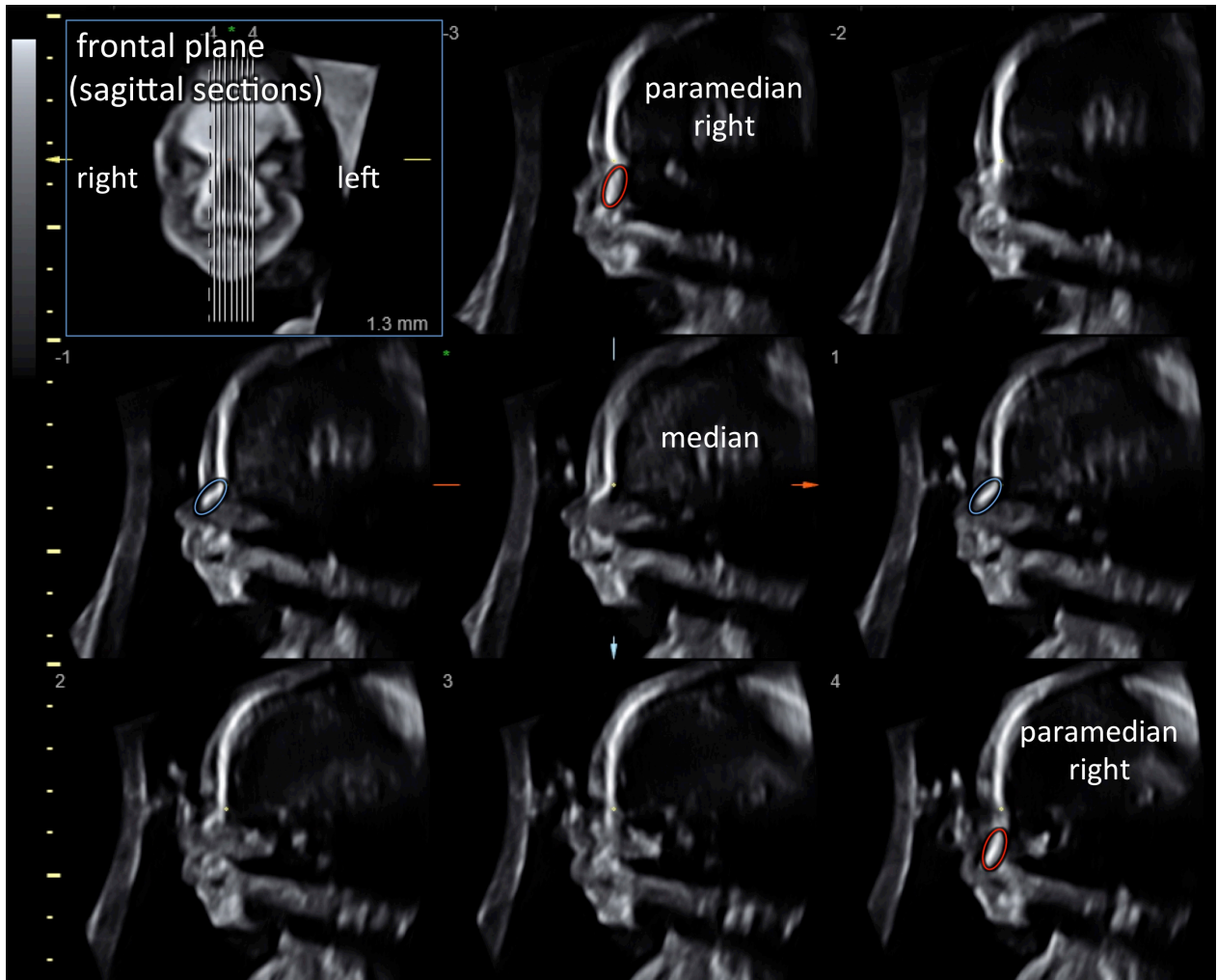


Figure S6 Tomographic imaging of a normal profile (same fetus as in Figures 2 and S5). Narrow spacing of adjacent sections permits differentiation between nasal bones (blue circles, images -1 and 1) and maxillary processes (red circles, images -3 and 4) on both sides.

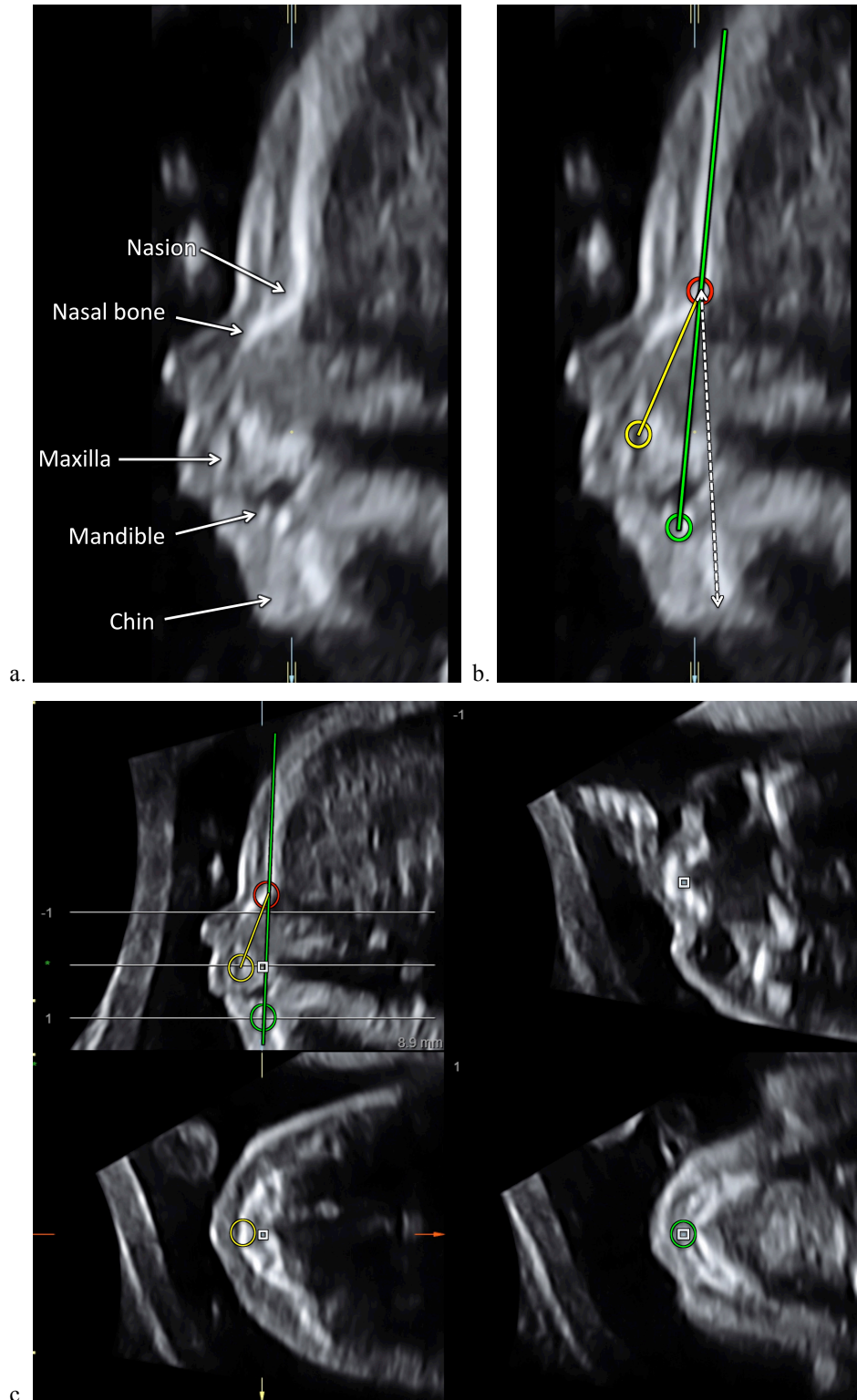


Figure 2 Normal fetal facial profile at 20 weeks, aligned and sectioned using three-dimensional ultrasound (same fetus as in Figures S5 and S6). (a) Midsagittal view, with osseous landmarks indicated. (b,c) Sagittal (b) and corresponding axial tomographic (c) images: red, yellow and green circles represent measurement point at nasion, maxilla and mandible, respectively. Green line is facial profile (FP) line. Because FP line passes through the frontal bone in this example, its position is ‘zero’. FP line in a receding frontal bone is ‘negative’ and in a prominent frontal bone is ‘positive’. Acute angle between line from nasion to maxilla (yellow line) and FP line is the maxilla-nasion-mandible angle. Dashed white double-headed arrow in (b) indicates facial height¹⁹, which corresponds to midface size.

Neurocranium and sutures

For analysis of the different parts of the fetal skull, three standard directions of insonation can be used: frontal, lateral and from the vertex.

For frontal insonation (fetus facing the transducer), a volume is acquired either from an axial view (e.g. with a cross-section of both orbits as the starting view) or from a sagittal view (with the profile view as the starting view). In such sweeps, the insonation angle is usually not suited to analysis of the secondary palate (see below). Frontal insonation usually displays the metopic suture and the facial and nasal bones (Figure S7). Depending on the setting for the render mode, skin or bone surface can be displayed (Figure 1). By selecting a render box that covers only one half of the face, this reconstructed half can be viewed without superimposition by tissues of the other half of the volume. The rendered volume can be inspected from different angles as well as from the outside or from the inside (Figure S8). An example of how to acquire, align and postprocess a volume to show the fetal facial bones and interactive reconstructions of a normal fetal skull are shown at <http://sf.fetal.ch>.

For lateral insonation, an axial volume is acquired with a starting level corresponding to the measurement planes of the biparietal diameter (with the ear facing the transducer; Figure 3). Lateral insonation displays frontal and parietal bones (as well as maxilla and mandible), coronal and lambdoid sutures and the squamosal and mastoid fontanel. The render box should include only one of the coronal sutures, i.e. one half of the skull at a time.

For superior insonation, a volume is acquired by placing the transducer over the vertex of the head. This allows analysis of the sagittal suture and the fontanel (Figure S9).

For analysis of the sutures, it is important to note that the image quality of a rendered view depends on the correct setting of the focal zone. If the rendered structures are at different depths, they will be displayed with different qualities, as resolution deteriorates distal to the focal zone; this may be overcome by acquiring volumes with different focal-zone settings.

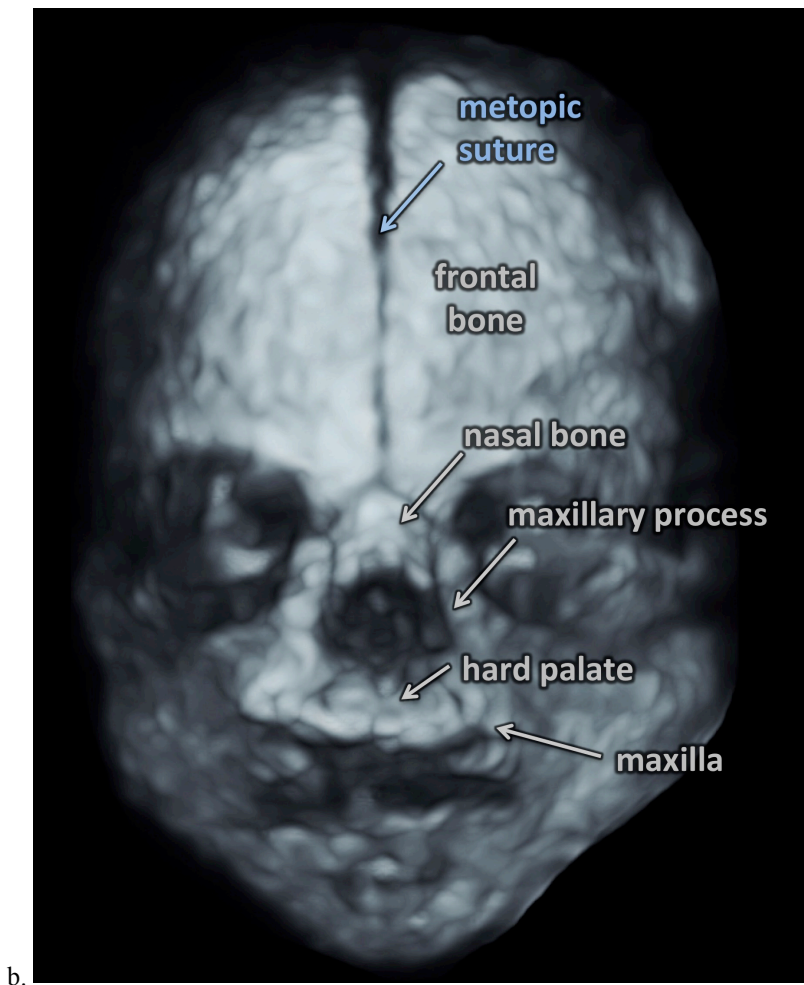
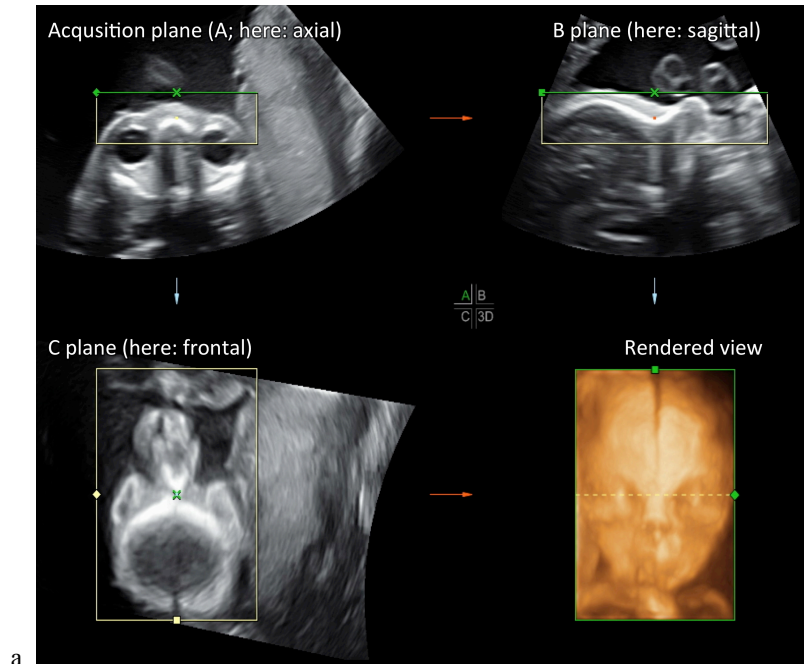
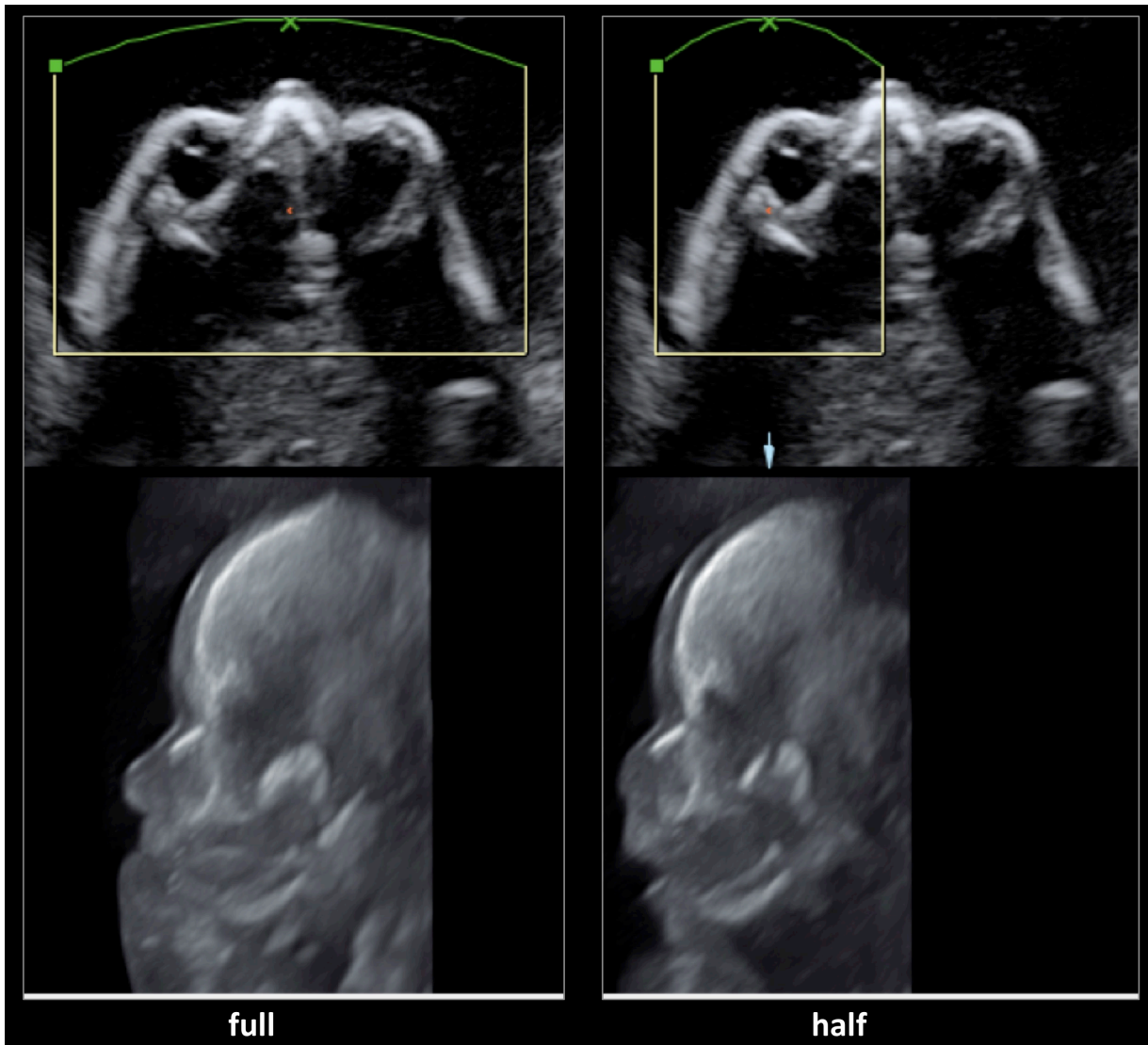
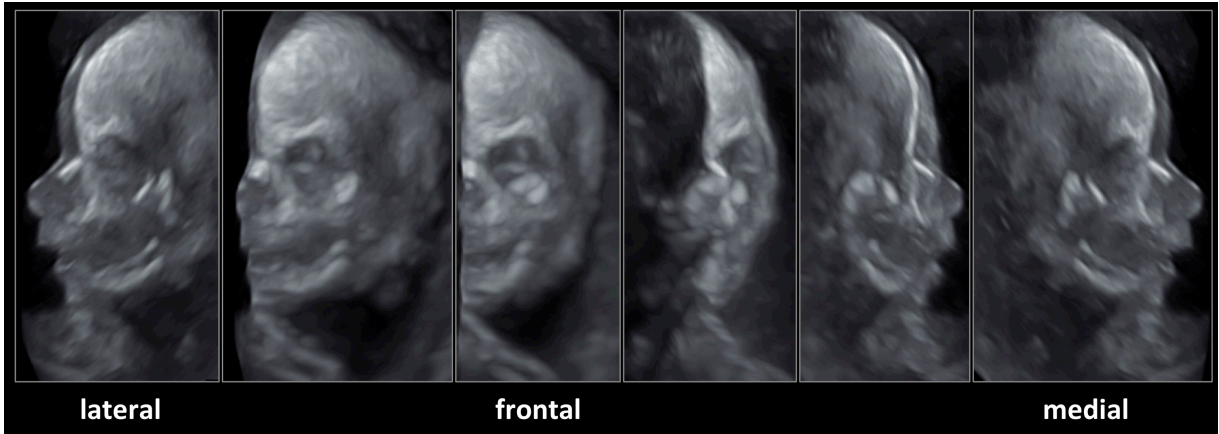


Figure S7 Three-dimensional ultrasound imaging in normal mid-trimester fetuses, following standard volume acquisition for the fetal face. (a) For volume acquisition the ultrasound beam is perpendicular to the anterior part of the brow (plane A, upper left panel). (b) Higher resolution image (different fetus) from the same insonation angle in a 25-week fetus, with bony structures enhanced using higher contrast and thresholds during postprocessing. Interactive reconstructions of a normal fetal skull and the skull of a trisomy-21 fetus are shown at <http://sf.fetal.ch>.

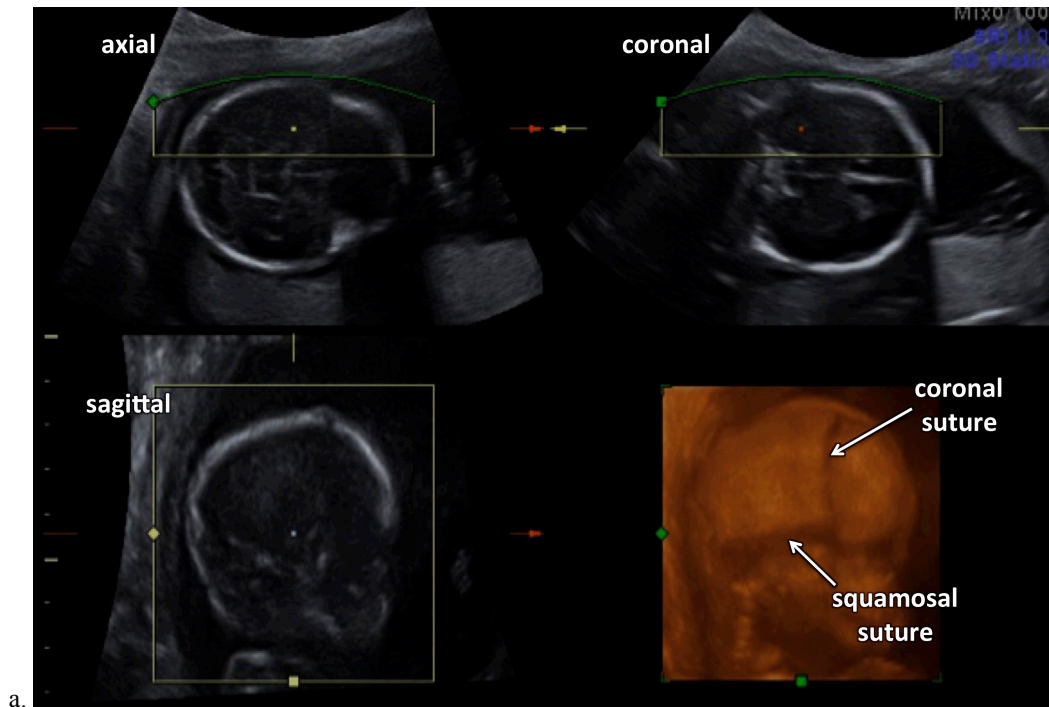


a.

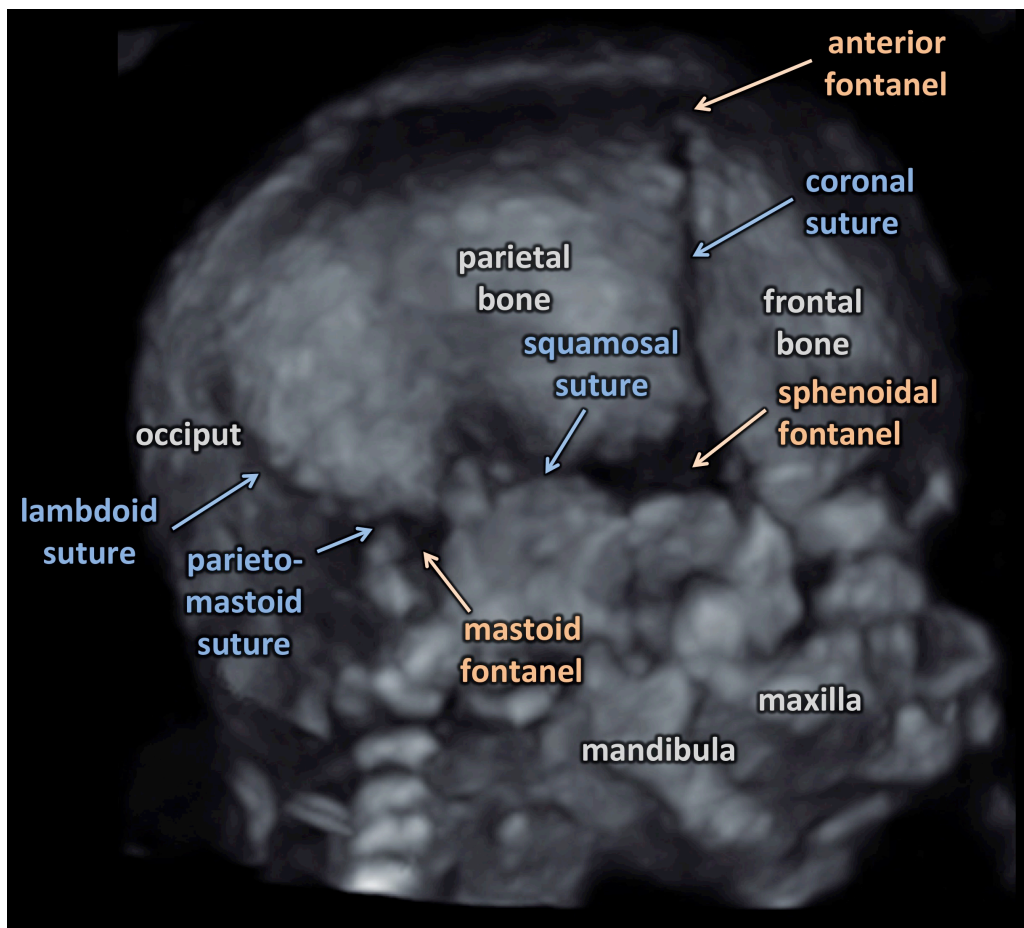


b.

Figure S8 Viewing options for frontally acquired three-dimensional ultrasound volume of normal mid-trimester fetal skull. (a) Render box can be adjusted to produce reconstruction of entire or only one half of the skull. The latter reduces superimposition of tissues and shows individual bones more clearly. (b) Viewing only the half skull, seen from different aspects (from the outside (lateral), frontal or from the inside (medial)), reveals more subtle anatomical details. An interactive reconstruction of a normal fetal skull is shown at <http://sf.fetal.ch>.



a.



b.

Figure 3 Three-dimensional ultrasound images following standard acquisition for coronal and squamosal sutures in a normal 20-week fetus. (a) Axial insonation with an ear facing the transducer. Focal zone is set in the near field. Note that render box includes only proximal side of cranium. (b) Higher resolution image using the same lateral insonation, with bony structures enhanced using higher contrast and thresholds during postprocessing.

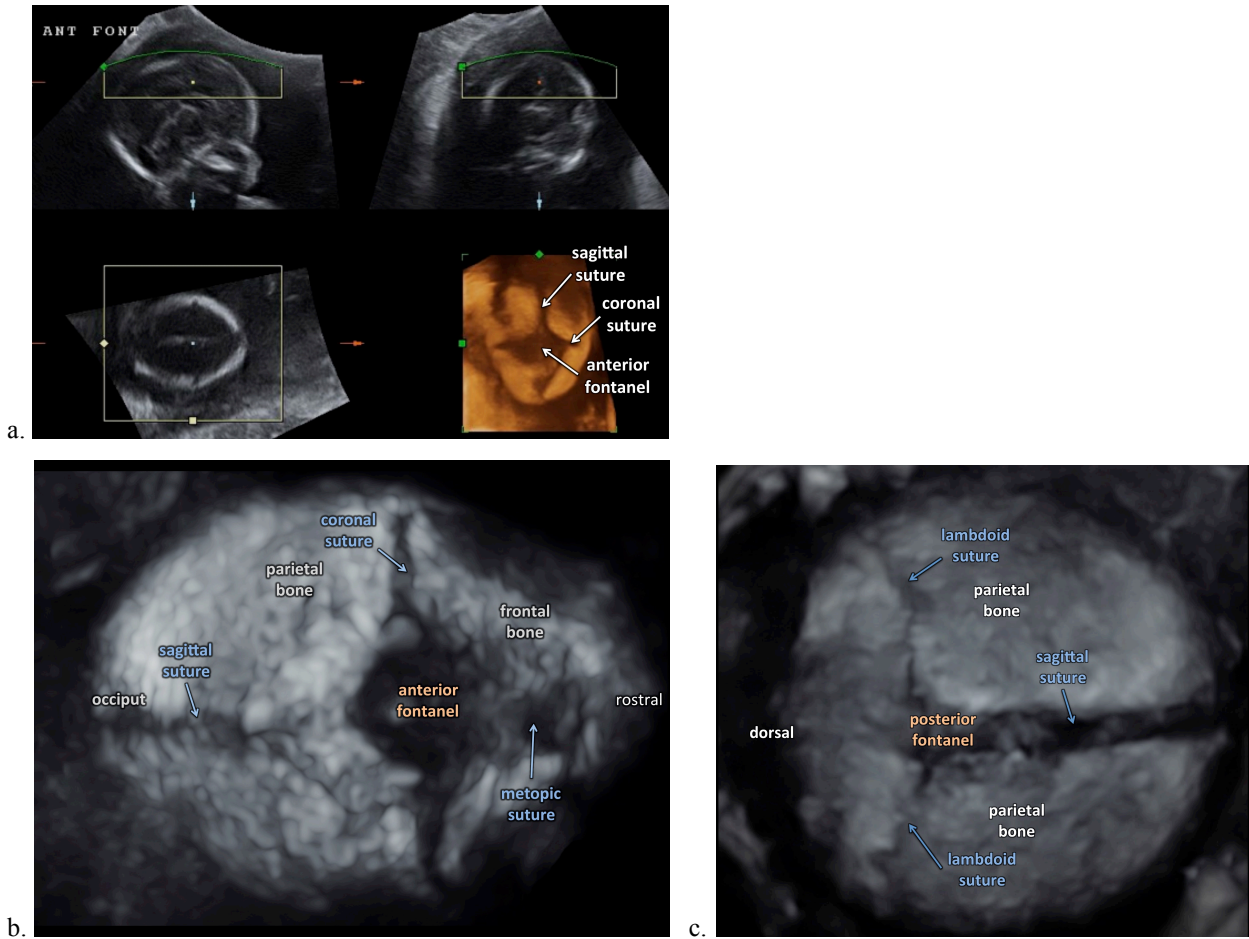


Figure S9 Three-dimensional (3D) ultrasound images following standard acquisition for sagittal suture and fontanelles in a normal 20-week fetus. (a) Sagittal insonation with anterior fontanel facing the transducer. Note that render box includes only upper half of the skull. (b,c) Higher resolution, annotated 3D image of normal 19-week fetal skull with anterior (b) or posterior (c) fontanel facing the transducer.

Hard and soft palate

Internal bones, i.e. those, such as the palate, which do not lie directly under the skin, are subject to shadowing by outer bones that lie in the path of the sound waves (Figure S3). Fetal position permitting, angling the transducer can avoid shadowing to optimize volume acquisition for a particular region. The alveolar ridge can be visualized easily in 2D and 3D when the fetus is facing towards the transducer, but the hard, and in particular the soft, palate requires an insonation that avoids shadowing from the alveolar ridge^{23,24} and the mandible. Such shadows may prevent clear imaging; ‘absence’ of a reconstructed ‘palate’ may be a typical 3D artifact (see Figure S13). Insonation with shadowing and with the correct technique are compared in Figure 4.

The posterior part of the hard palate and the soft palate are curved structures, making rendering difficult even when the correct insonation angle is used during volume acquisition. Placing a curved reconstruction line and using volume contrast imaging may overcome this limitation (Figure 5), provided the secondary palate is not shadowed. Scrutinizing the volume on three planes in multiplanar display enables confident recognition of such shadowing.

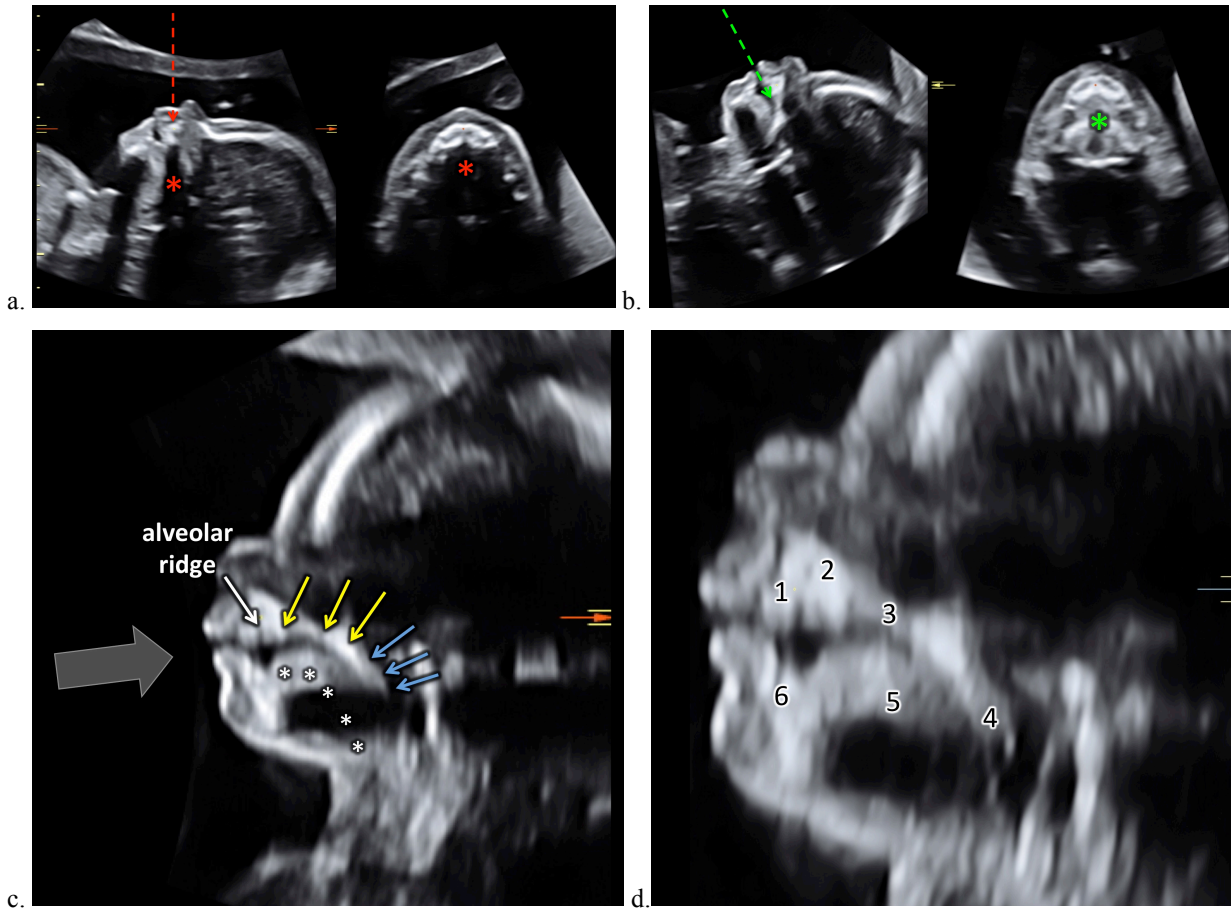


Figure 4 Insonation of the fetal palate. Angling the transducer in the midsagittal plane overcomes shadowing of internal structures. (a) Good insonation angle for profile and alveolar ridge, but shadowing of secondary palate by the alveolar ridge (dashed red arrow). Note black space (shadow; red asterisk) inside the alveolar ridge that precludes assessment of the secondary palate. (b) Another volume, acquired with an insonation angle appropriate for alveolus and palate. Placing the transducer below the fetal chin, the shadow of the alveolar ridge is now above the secondary palate, exposing the entire hard palate (green asterisk). (c) Magnified and upright version of the correctly acquired volume (from b), showing hard (yellow arrows) and soft (blue arrows) palate and tongue (asterisks). In the normal resting state, the tongue and the hard and soft palate close the oral cavity against the pharynx, as seen here. Large arrow indicates insonation direction. (d) Higher-resolution image of fetal maxilla, palate and neighboring structures, showing the alveolar ridge of the palate (1), vomer (2), horizontal plate of the palate (3), soft palate and uvula (4), tongue (5) and mandible (6).

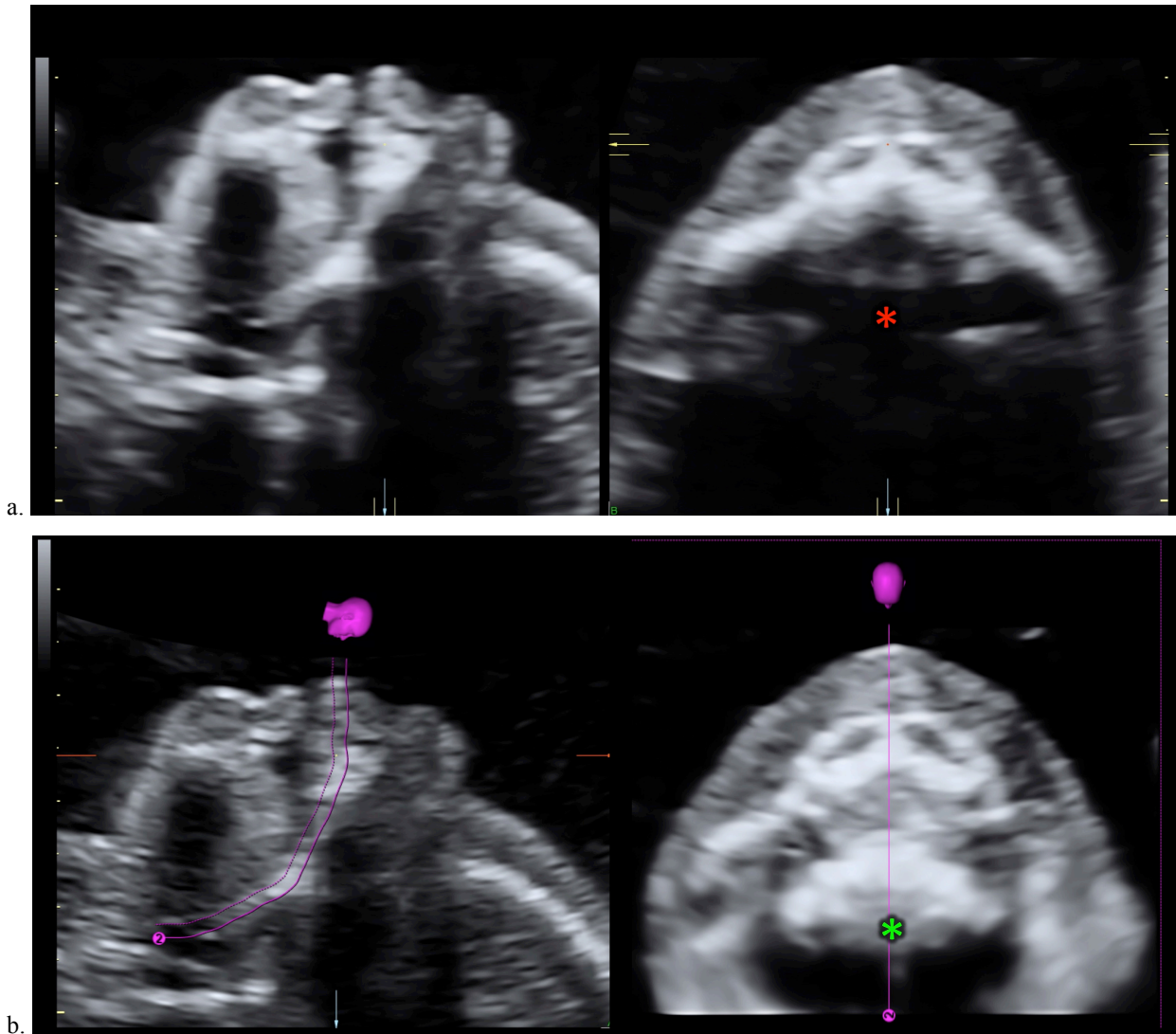


Figure 5 Reconstruction of hard and soft fetal palate, using a curved plane (both reconstructions from same volume). (a) A straight plane is used. Only the anterior part of the curved structure of the hard palate is seen and none of the soft palate (red asterisk) is displayed in the right image, despite the absence of shadowing. (b) Using a curved reconstruction plane, the entire hard and soft palate (green asterisk) down to the uvula can be seen.

Nasal bone

The nasal bones are among the small bones of the fetal skull, and have been studied using 3D-US²⁵. Confirmation of their presence, both left and right, in the three orthogonal planes on multiplanar or rendered imaging can be helpful (Figure S10), in particular in the first trimester²⁶. Volumes should be acquired from the sagittal or axial planes of the face.

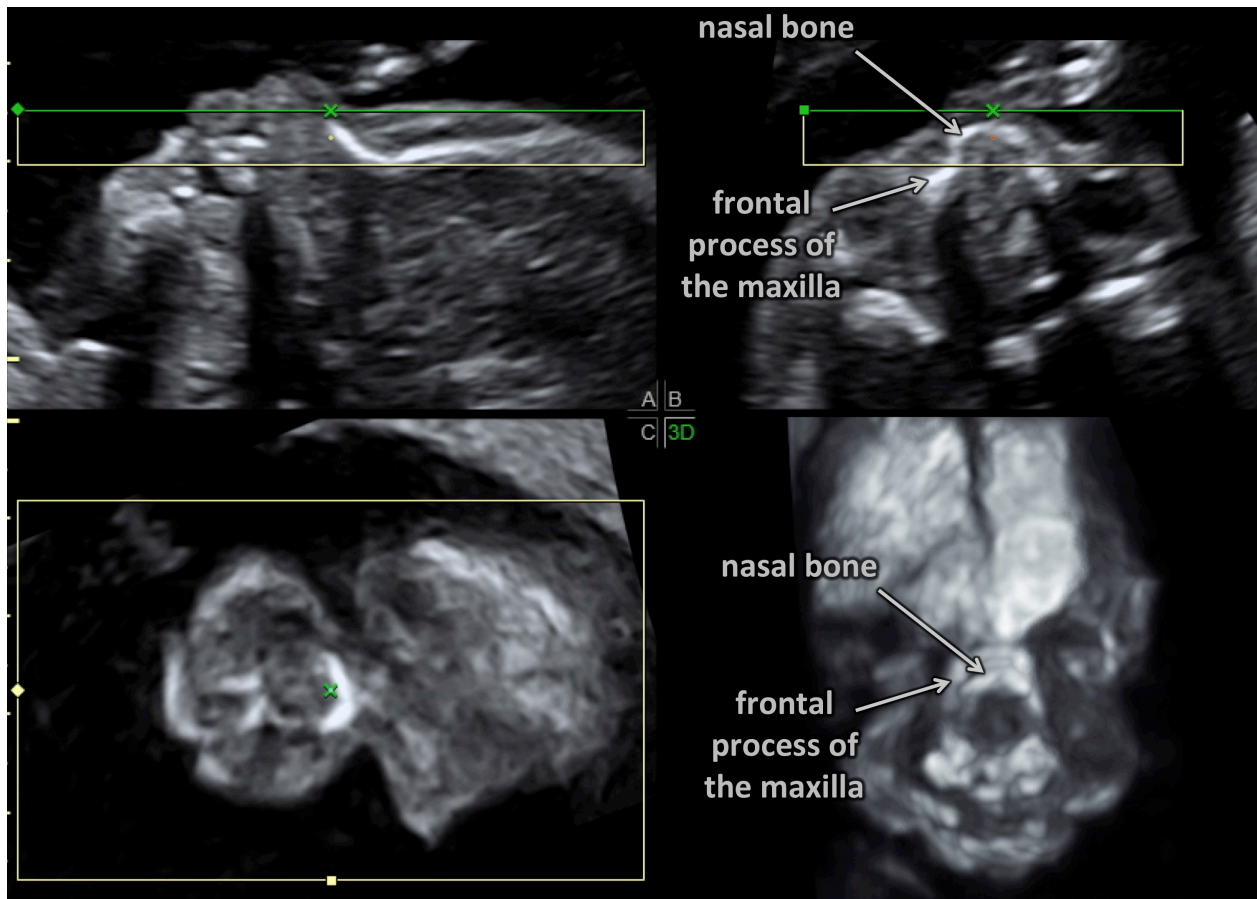


Figure S10 Normal fetal nasal bones in multiplanar and rendered displays. An interactive reconstruction of a normal fetal skull is shown at <http://sf.fetal.ch>.

Skull base

Other cranial bones have also been studied by 2D- and 3D-US to assess their development during pregnancy. The skull base can be studied from different insonation angles, but not all bones in the skull base may be seen due to shadowing or reflections²⁷⁻²⁹ (Figure S11). Dysplasia of the skull base can occur with many conditions and can be detected by both 2D- and 3D-US³⁰.

The tympanic ring provides the osseous framework surrounding the tympanic membrane; it can be demonstrated by 3D-US in mid-gestation (Figure S12), but only before full ossification of the petrous bone occurs³¹. Dysplasia or aplasia of the tympanic ring may result in congenital conductive hearing loss and may be related to genetic syndromes.

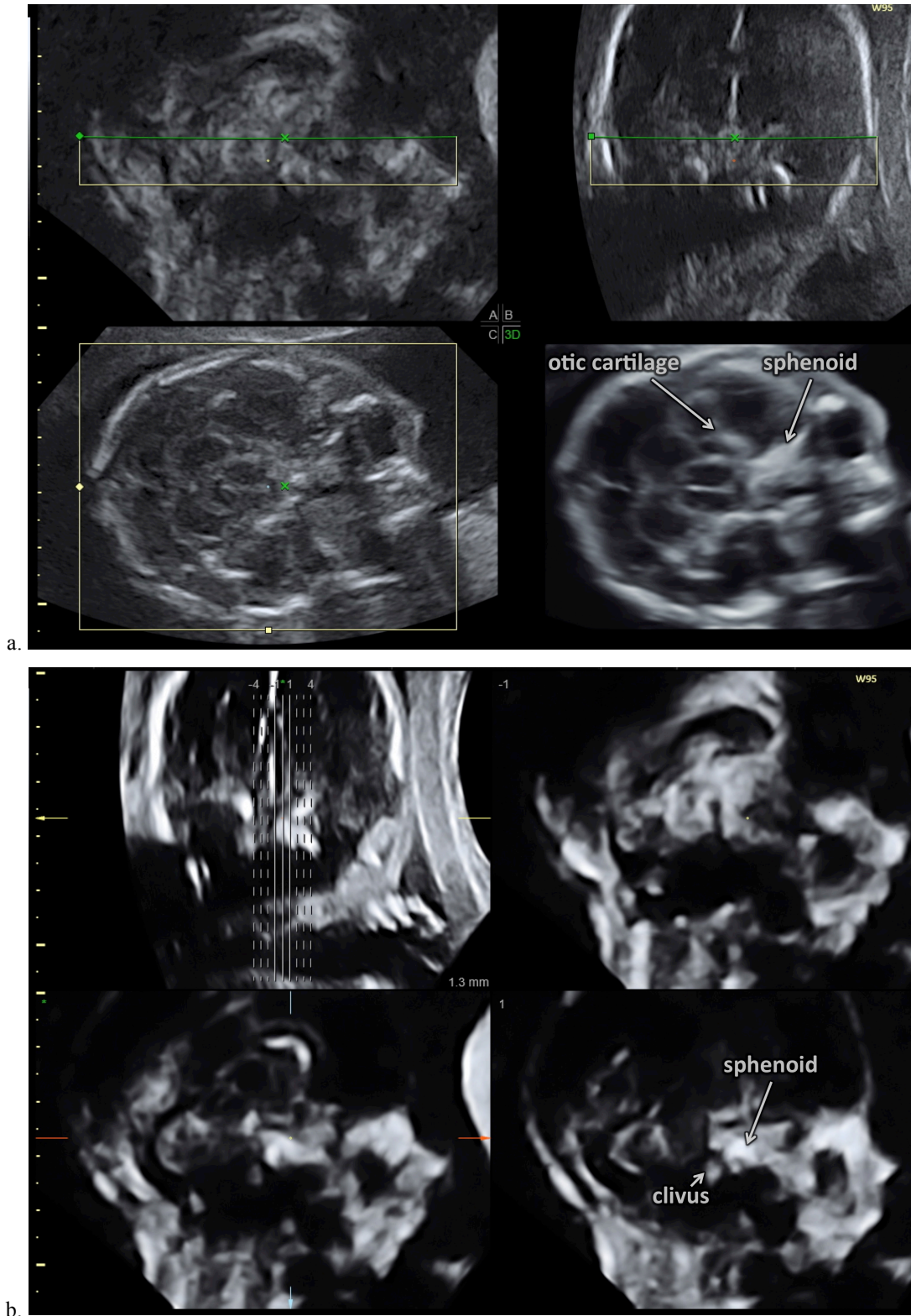


Figure S11 Normal fetal skull base displayed using three-dimensional ultrasound. Inner skull bones, such as the skull base, are often shadowed by external bones. Often only partial reconstruction of individual bones is possible. Sphenoid bones and otic cartilages can be seen in an axial plane (a) and sphenoid bone and clivus can be demonstrated in a (para)sagittal section (b)²⁷.

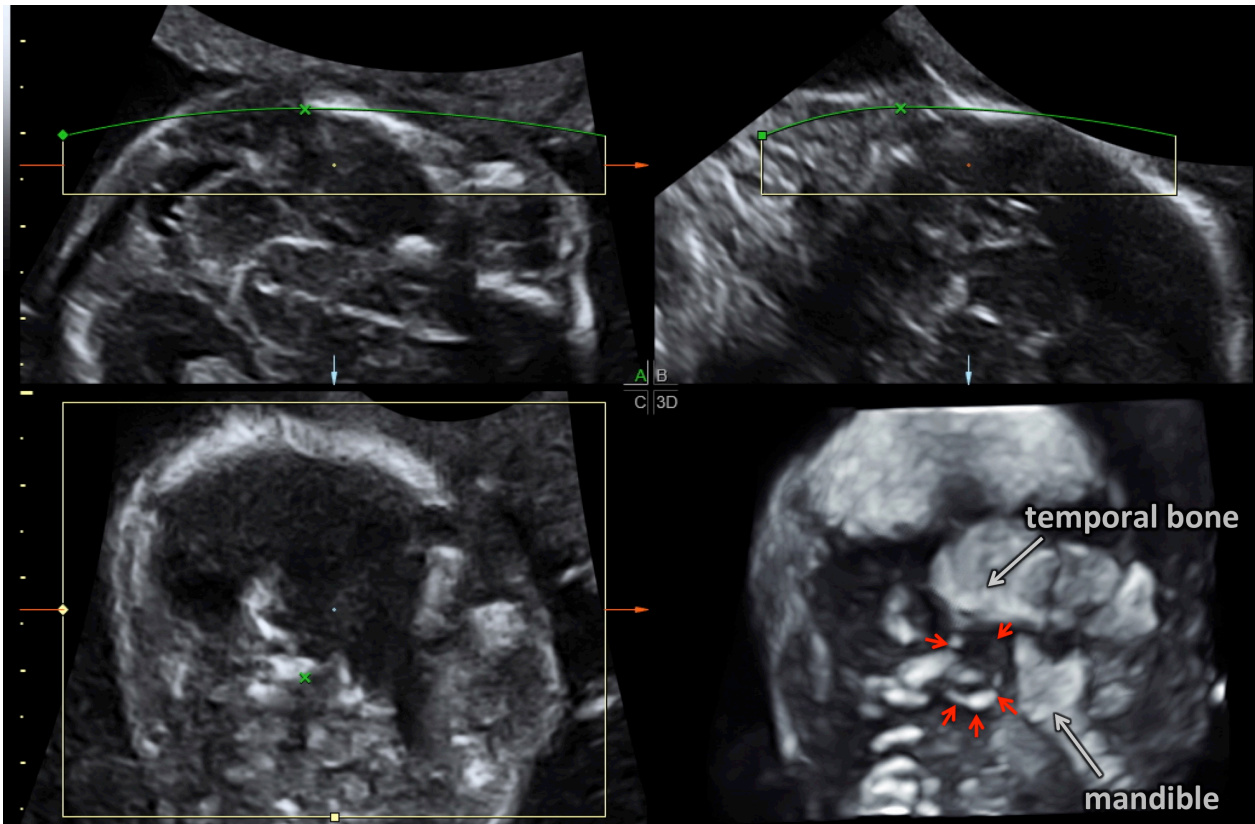


Figure S12 Three-dimensional ultrasound imaging of the tympanic ring (according to Leibovitz *et al.*³¹), which can be reconstructed from an (early) mid-trimester volume, acquired from angled lateral insonation.

Pitfalls and artifacts

3D-US is subject to the same artifacts as 2D-US, but may also present additional artifacts related to volume acquisition and visualization. Sometimes 3D-US will enhance 2D artifacts during volume data manipulation. The potential consequences of diagnostically significant artifacts include mimicking of abnormal development, masses or missing structures, thus necessitating careful study before diagnosis is reached³². In the example of a normal fetus shown in Figure S13a, shadowing causes the reconstruction to appear incomplete in a region that could be either a true positive (a true cleft palate) or a false positive (a normal palate with a reconstruction artifact).

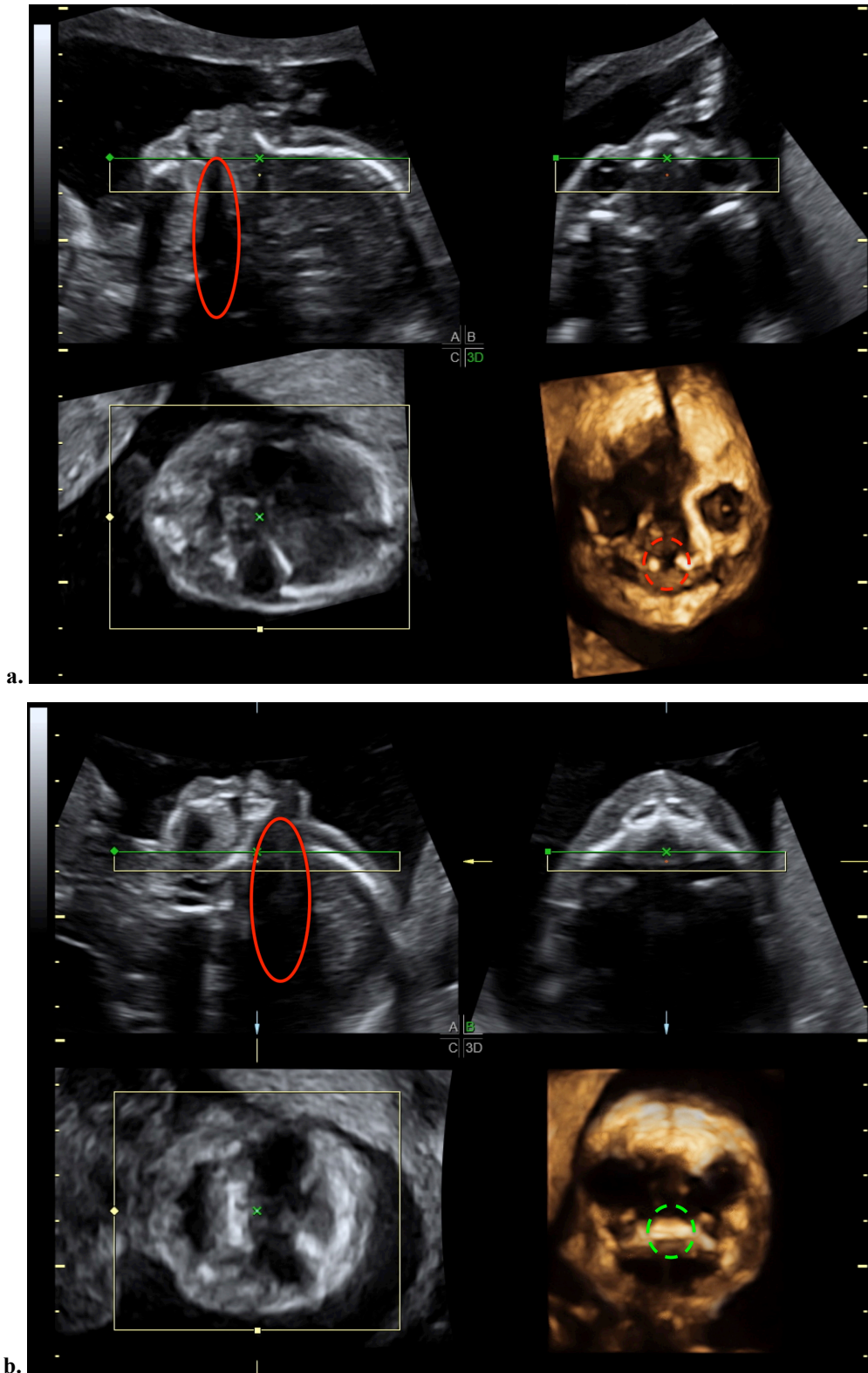


Figure S13 Two facial volumes acquired frontally from the same normal fetus, but from different insonation angles. (a) Front, nose and maxilla are aligned horizontally, a usual orientation from which to produce a fetal profile image. The volume acquired from this insonation angle contains a shadow of the alveolar ridge that obscures the secondary palate completely (red oval); the resulting volume reconstruction (bottom right) has an apparent defect in the hard palate (red dashed circle). (b) Correct insonation, tilted and with a caudal starting point, moves the palate out of this shadow (red oval); the three-dimensional reconstruction now correctly shows the intact secondary palate (green dashed circle).

Clinical examples

The following section illustrates the general principles outlined above, using clinical cases.

Abnormal profile

3D surface rendering may demonstrate skull, facial and associated skeletal anomalies impressively (see Figure S19), but multiplanar or tomographic displays are more suitable for a systematic analysis of the fetal face. In a multiplanar display of a perfectly aligned facial volume, the anatomical landmarks can be identified with confidence (Figures 2, S5 and S6); 2D imaging is prone to malalignment that goes unnoticed³³, leading to possible misdiagnoses^{34,35}. Using multiplanar display, the profile can be assessed for a prominent or receding forehead, a small nose or an abnormal chin size or position, eliciting typical features of different pathological entities (Figures 6 and S14). Multiplanar analysis also allows quantitative assessment of individual bones, such as the maxilla and the mandible, which can be small or positioned abnormally in a number of genetic conditions^{17,36-38}.

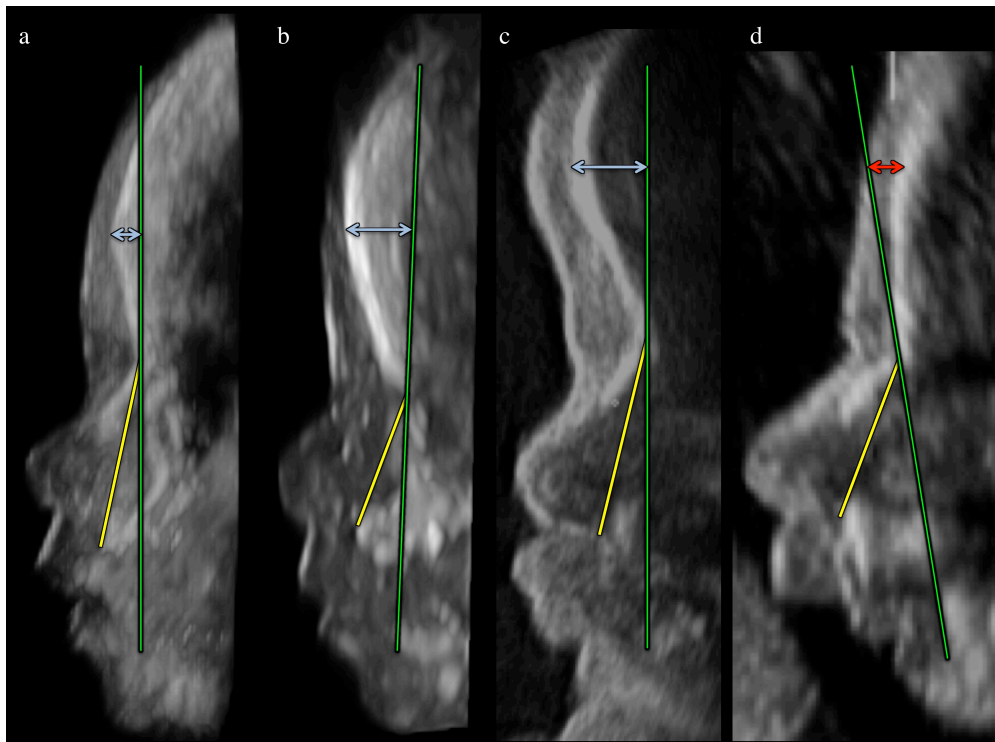


Figure 6 Anatomically aligned midsagittal sections from three-dimensional ultrasound imaging in four different fetuses. (a) Normal profile with a normal maxilla-nasion-mandible angle (MNM) and a normal, mildly positive facial profile (FP) line. (b) Down-syndrome fetus, showing small mandible, depressed nasion and prominent forehead, which cause an increased MNM angle and a more positive FP line value. Note, the height of the midface (from nasion to mandible) also appears smaller than the part above the nasion (midface hypoplasia). (c) Fetus with achondroplasia, showing marked protrusion of frontal bones (frontal bossing), leading to increased FP line value. (d) Fetus with micrognathia, showing small, receding mandible, leading to markedly increased MNM angle and accentuation of receding forehead (negative FP line). Note, microcephaly (with or without normal mandible) also produces negative FP line. Interactive reconstructions of a normal fetal skull and profile and of a skull in trisomy 21 are shown at <http://sf.fetal.ch>. Green line, FP line; yellow line, line from nasion to maxilla; acute angle between green and yellow lines, MNM angle; blue arrow, positive FP line; red arrow, negative FP line.

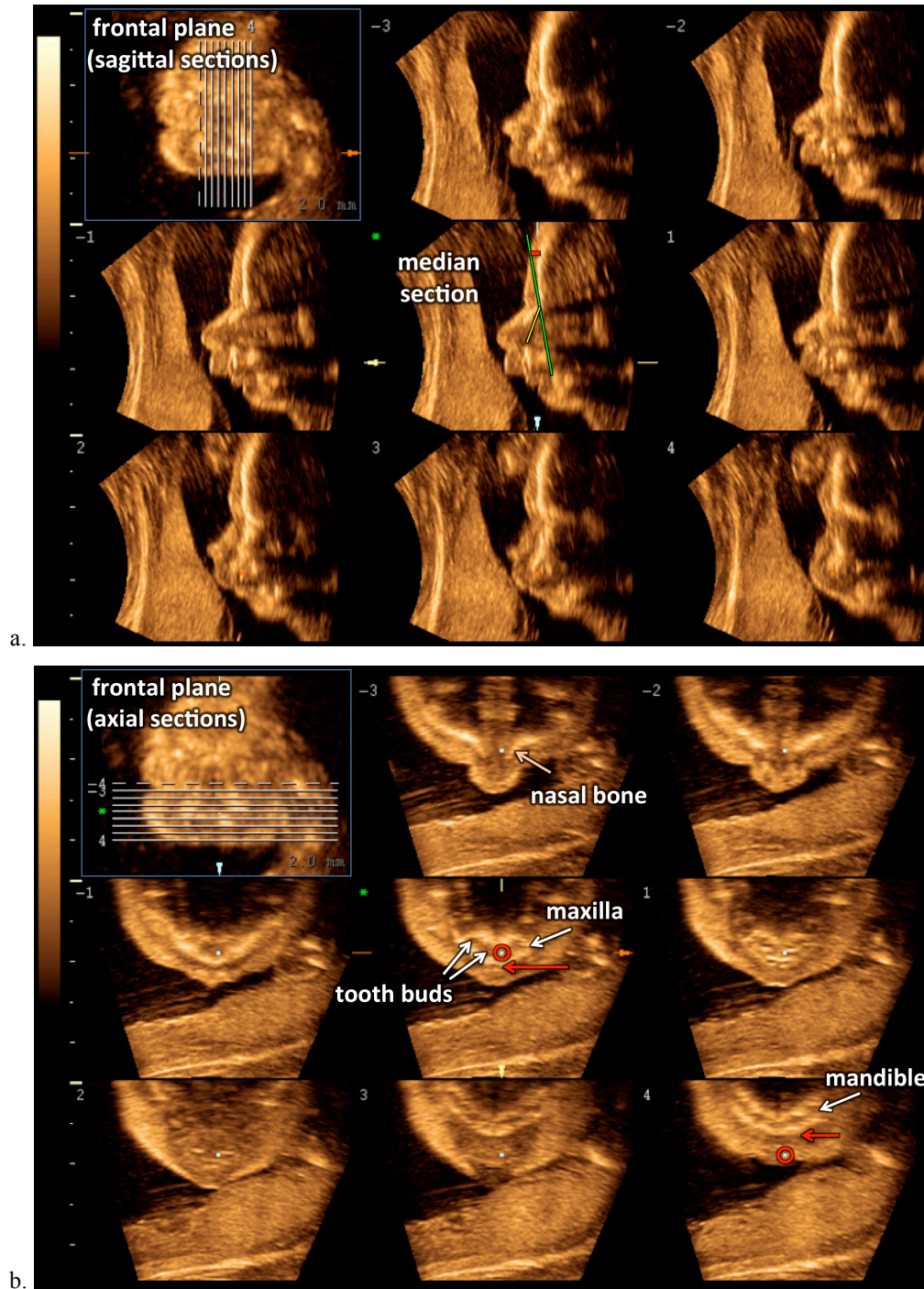


Figure S14 Tomographic imaging from a single ultrasound volume from a mid-trimester fetus with micrognathia. Volume had been acquired from frontal insonation and aligned anatomically. (a) Tomographic imaging in sagittal plane (spacing, 2 mm), showing extent of micrognathia best in midsagittal plane. Facial profile (FP) line (green line) is negative (red line) and maxilla-nasion-mandible angle is enlarged due to micrognathia. In no parallel plane can a normal profile be seen. (b) Same volume, formatted to display parallel axial planes (spacing, 2 mm). The eight panels show axial sections demonstrating nasal bones, maxilla (with tooth buds) and mandible. Note, reference dot (highlighted by red circle) lies central in the maxilla, but far frontal to the mandible due to micrognathia.

Missing or hypoplastic nasal bones

The nasal bones may ossify late or incompletely in fetal trisomy 21, and can be used as a risk marker in Down-syndrome screening³⁹⁻⁴¹. They can be visualized using 3D-US. However, in small fetuses, optimal 2D image quality is crucial for correct 3D reconstruction⁴². In suspected

abnormal cases, care must be taken to visualize both nasal bones and to note not only whether there is ossification of the nasal bones, but also if they appear normal in ossification or length, hypoplastic or entirely without ossification⁴³. As the nasal bones are small and can be obscured by neighboring bones, they are seen more readily if the focal zone is at the level of the nasal bone, if the render box covers only the frontal-most part of the skull and when the bone-rendered view is viewed from the side (Figure S15).

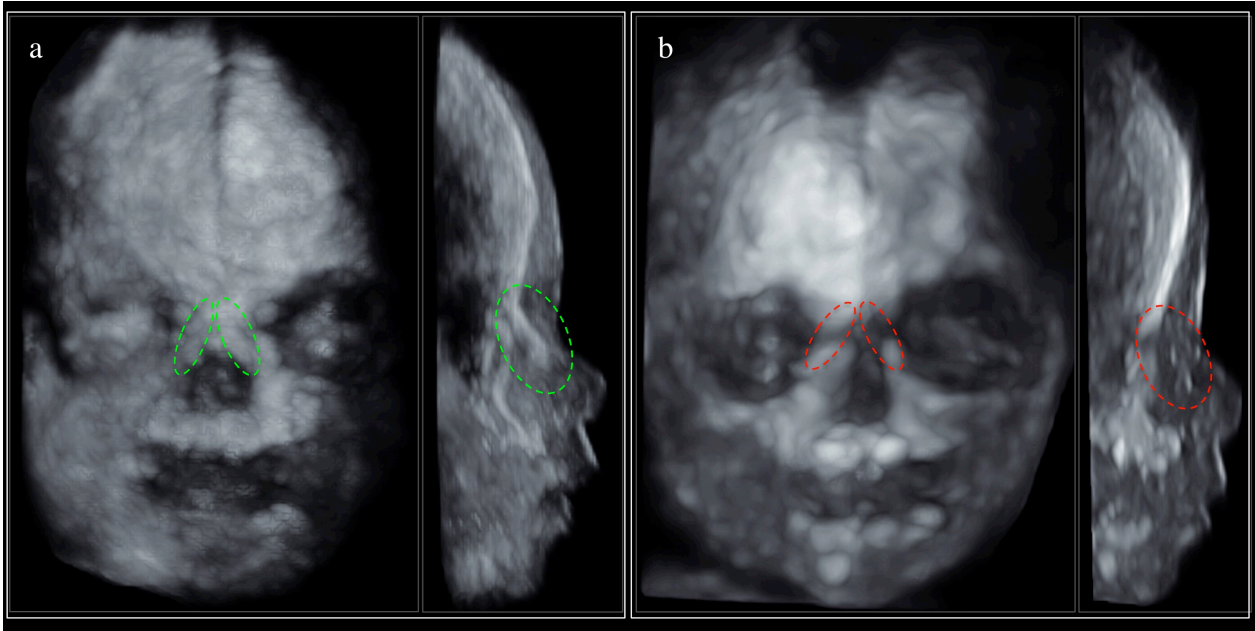


Figure S15 Frontal and lateral views of fetal facial and nasal bones in: (a) a normal fetus at 22 weeks and (b) a 22-week fetus with trisomy 21 with non-ossification of both nasal bones. Both volumes were acquired from a frontal insonation, aiming for perpendicular alignment of the nasal bone region with regard to the transducer; the resulting bone reconstruction was then rotated to provide a lateral view. Green and red ovals indicate locations of the nasal bones. Note that the nasal region is clearer in both laterally rotated views, that, in the trisomy 21 fetus (b), absence of the nasal bones is more easily seen, and that the profiles (both osseous and bony) are slightly, but characteristically, different. Multiplanar display can also be used to move the reference dot on the suspected nasal bone to verify that it is in fact the nasal bone and not the frontal process of the maxilla. Interactive reconstructions of a normal fetal skull and of a skull in trisomy 21 are shown at <http://sf.fetal.ch>.

Cleft lip and palate

The most common facial clefts are of the lip and palate, which occur in approximately 1 in 500 births⁴⁴. 3D-US can be used in the diagnosis of orofacial clefts affecting the soft tissue of the lips and palate as well as the alveolar ridge and secondary palate⁴⁵⁻⁴⁸.

External clefts can be present as a cleft of the lips only (cleft lip, CL), as cleft lip and alveolus (CLA) or extending from the lips and alveolar ridge towards the inside, including a cleft in the hard palate (cleft lip and palate, CLP). External clefts can be unilateral, bilateral or median. In a perinatal study using 3D-US, the most common external clefts were CLP (77%), followed by CL (19%) and CLA (4%). 3D-US had a high degree of accuracy (97%) in predicting the correct type⁴⁹.

An isolated CL can be demonstrated along the intact alveolar ridge using 3D-US. Figure S16 shows a volume from a fetus with CL, formatted to display the soft tissue defect as well as the intact alveolar ridge.

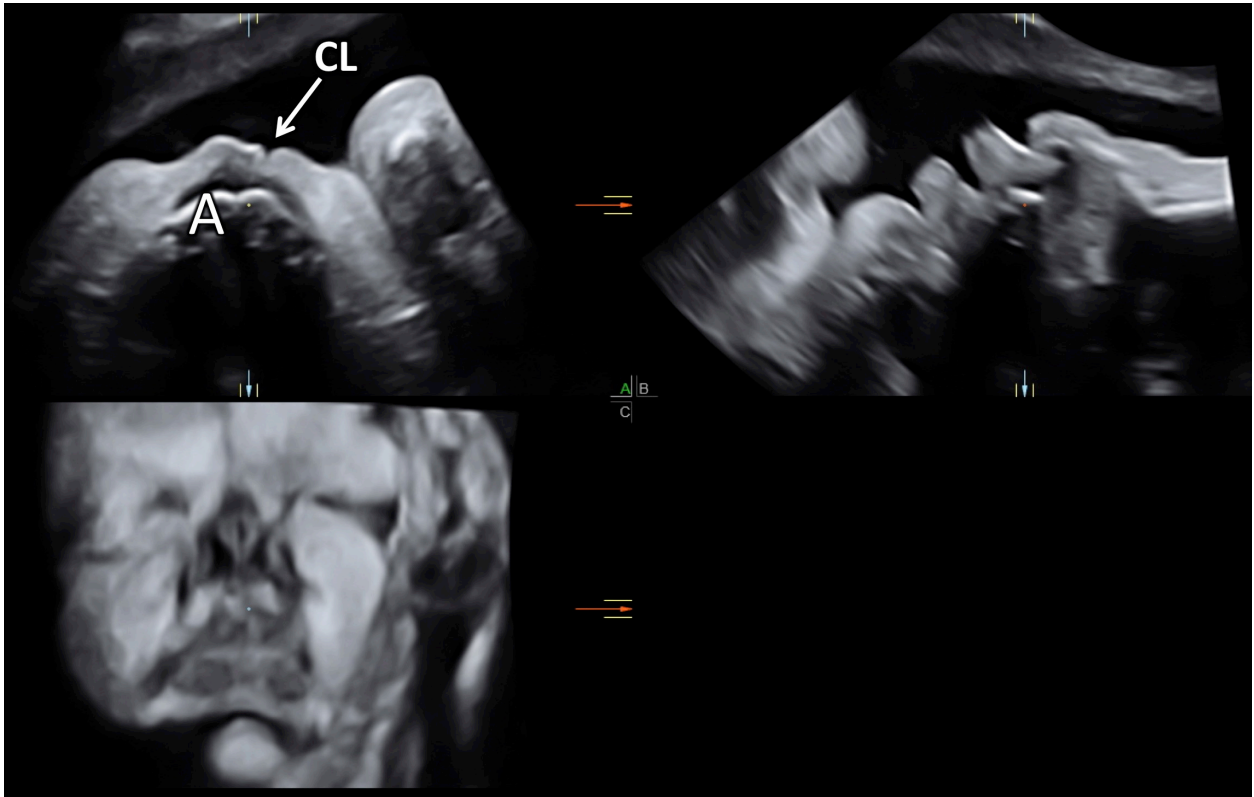


Figure S16 Isolated unilateral cleft lip (CL). The multiplanar display is aligned to show the axial section of the intact alveolar ridge (A) at the level of the small defect in the lip.

In isolated cleft palate (CP), an internal cleft and embryologically different entity, the lip and alveolus are intact. CP is always midline, ranging from a cleft uvula to a cleft soft and hard palate. Isolated CP accounts for a considerable number of all orofacial clefts^{47,50}. The diagnosis of CP is challenging and is usually missed; however, observing the correct insonation angle (Figure 4) and 3D reconstruction technique (Figure 5) may enable diagnosis^{48,51}.

Different approaches have been proposed for 3D rendering, mainly of the bony component of maxillary clefts, including viewing the rendered surface from the back ('reverse-face view'), using an upside-down view of the roof of the oral cavity ('flipped-face view', surface-rendered oropalatal (SROP) view), or scrolling the fetal head back and forth through the render box^{47,52-54}. The combination of an oblique insonation angle and the correct rendering approach, ideally in the presence of at least a small fluid rim between the tongue and the palate, provide adequate imaging^{53,55-57}. Figure 7 shows a volume from a fetus with CLP, rendered to display the bony defect. Note that the vomer becomes visible as the entire secondary palate is missing.

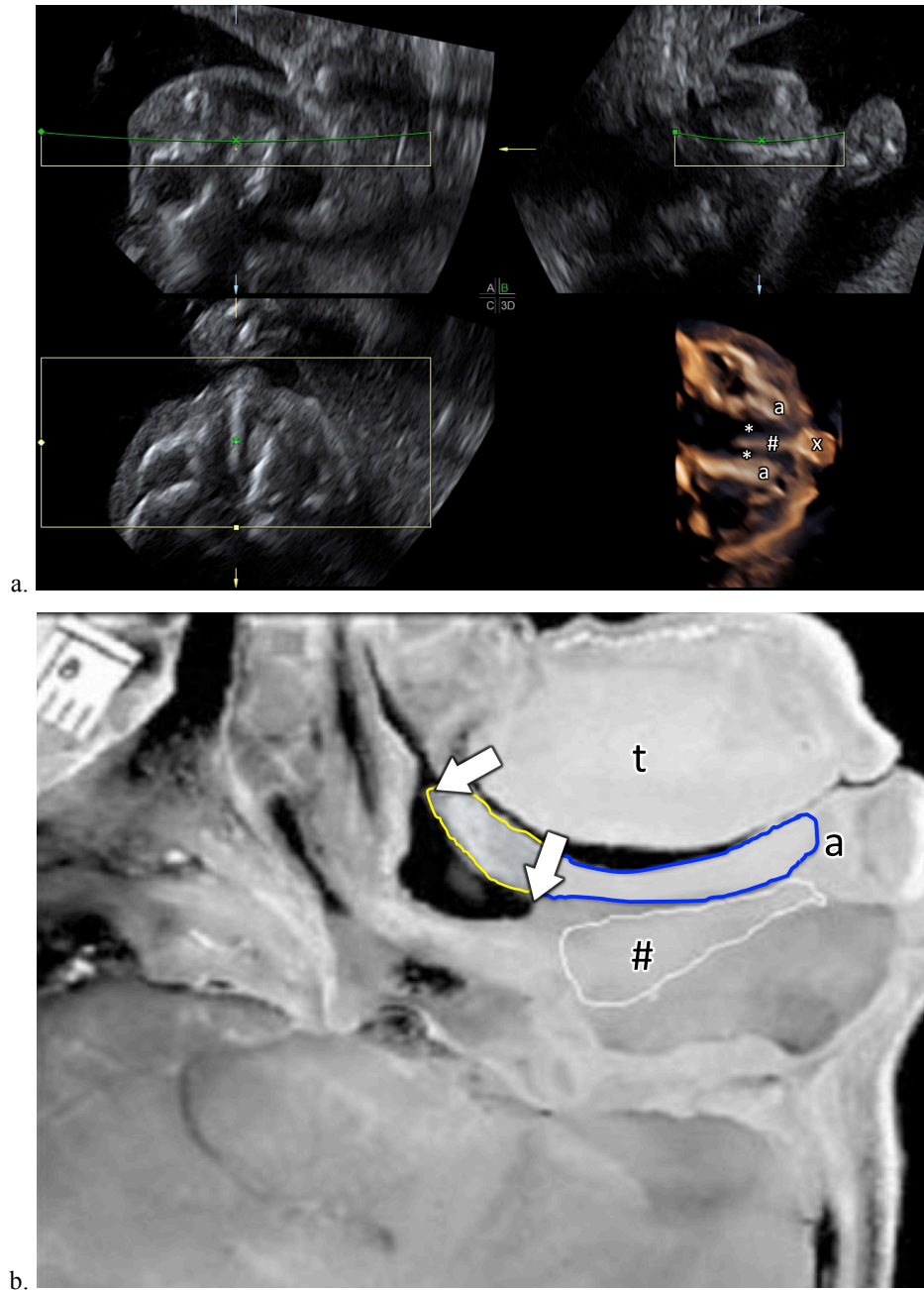


Figure 7 Bilateral cleft lip and palate (CLP). Multiplanar and rendered view. (b) For comparison, a normal anatomical specimen (midsagittal section of a normal fetal face) is shown in same orientation as that in Panel B in (a). Fetal vomer (#, white outline), hard palate (blue outline) and soft palate (arrows, yellow outline) are shown (modified from image provided by Professor Gonzalo Moscoso). X, premaxillary mass (typical for bilateral CLP); a, interrupted alveolar ridge; t, tongue; *, cleft palate; #, vomer bone (visible separate from the hard palate in large clefts).

Skull anomalies in genetic skeletal disorders

There are many genetic disorders that affect the skeleton, some of them including the skull. According to the 2015 revision of the nosology and classification of genetic skeletal disorders⁵⁸, there are 42 groups with a total of 436 skeletal disorders, involving 364 identified genes. The contribution of 3D-US in promoting the prenatal diagnosis of skeletal dysplasia is not yet proven, due to the rarity of these conditions. So far, only a few cases of skeletal disorders

involving the skull have been described by 3D-US; we include here several cases categorized according to the current classification⁵⁸.

Group 1, the fibroblast growth factor receptor 3 gene (FGFR3) chondrodysplasia group, includes seven clinical conditions, comprising thanatophoric dysplasias (TD) Types 1 and 2 and achondroplasia, that are detectable by prenatal US and may exhibit skull anomalies⁵⁹.

Thanatophoric dysplasia

TD is a micromelic (short-limbed) dwarfism caused by a mutation in the FGFR3 gene. It is characterized by marked shortening of the long bones and (in 60% of cases) a large head^{59,60} with an abnormally prominent forehead (frontal bossing) and midface hypoplasia (Figure S17). Marked hypergyration of the temporal lobe (temporal lobe dysplasia) is always present and is also a consequence of certain FGFR3 gene mutations⁶⁰. In TD Type 2, characteristic bulging of the cranial bones may be seen, giving the head a clover-leaf shape (best seen in coronal views).

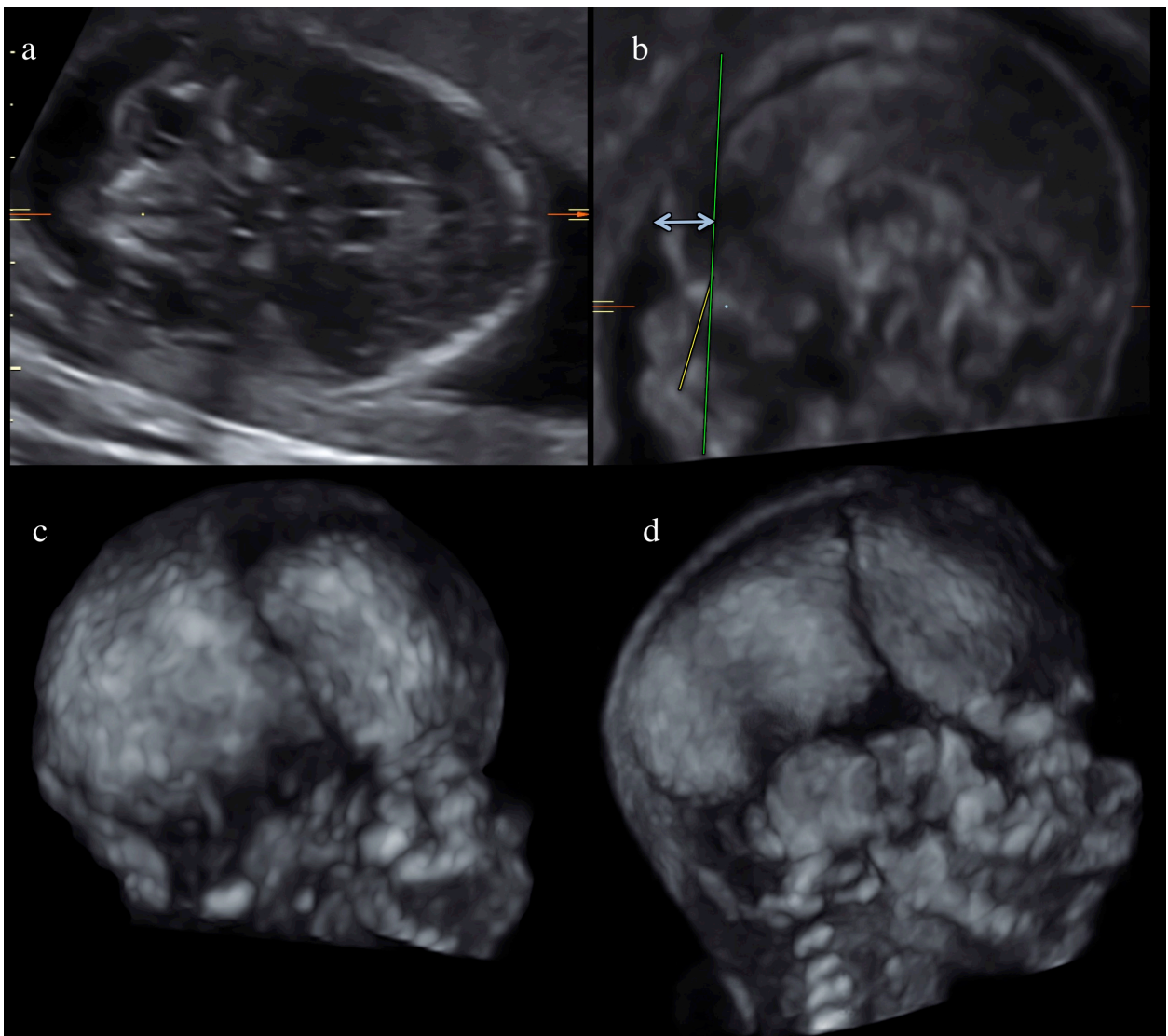


Figure S17 Abnormal profile and face of a fetus with thanatophoric dysplasia (TD) type 1 at 15 weeks, analyzed using three-dimensional ultrasound. (a) Axial view of the skull at the level of the orbits and (b) abnormal profile analyzed using multiplanar imaging. In (b) the green facial profile line shows marked frontal bossing (double-headed arrow). (c) Skull-rendered image (lateral insonation); note depressed nasion and mid-face hypoplasia. (d) Correspondingly aligned normal skull for comparison.

Achondroplasia

Achondroplasia, which also belongs to the FGFR3 chondrodysplasia (Group 1), is one of the most common non-lethal skeletal dysplasias⁵⁹. Affected fetuses can exhibit a number of skeletal anomalies⁶¹. The appearance of the skull and face typically includes macrocephaly with frontal bossing and midface hypoplasia. It should be noted that features such as short long bones and the characteristic profile usually develop only after 20 weeks, i.e. too late for the routine mid-trimester anatomy scan. When assessing the fetal profile, the multiplanar view can be very useful to display a correctly aligned profile (Figure S18) and rendered views also show typical features of the head and extremities (Figure S19). We suggest using 3D-US for fetuses with short long bones and suspicion of frontal bossing. Aligning the volume anatomically so that the fetus is upright and displayed symmetrically permits differentiation of an oblique image of a normal fetus and true frontal bossing.

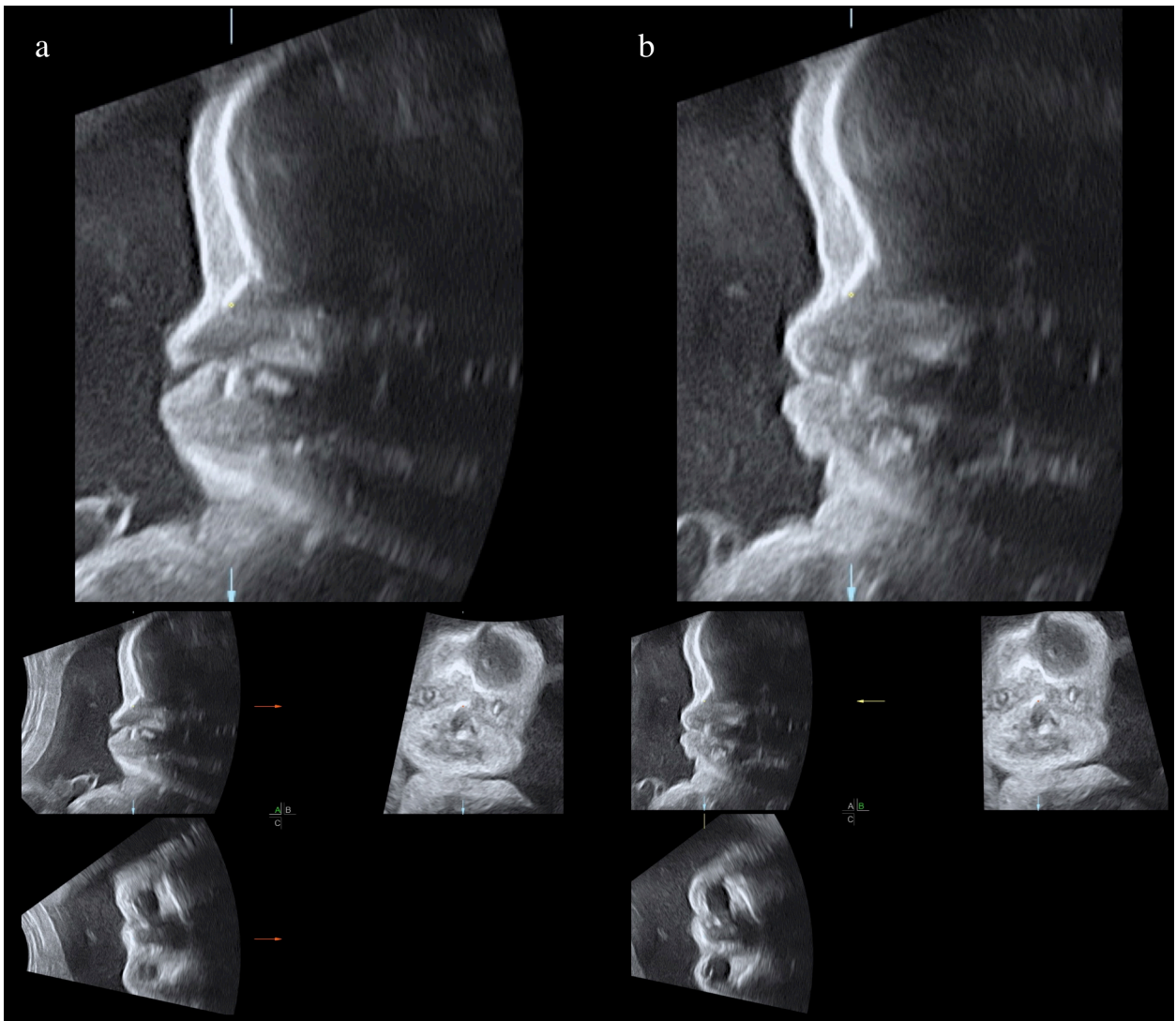


Figure S18 Achondroplasia and the effect of incorrect anatomical alignment: profile views of a fetus with achondroplasia (29 weeks), extracted from the same volume (top row), with one not anatomically aligned (a) and one aligned correctly (b). The most salient feature, frontal bossing, is better appreciated in the correctly aligned view (b). In this example, slight rotation (recognizable in the frontal plane in (a)) makes the characteristic profile less clear, but three-dimensional ultrasound imaging permits correct alignment (b).

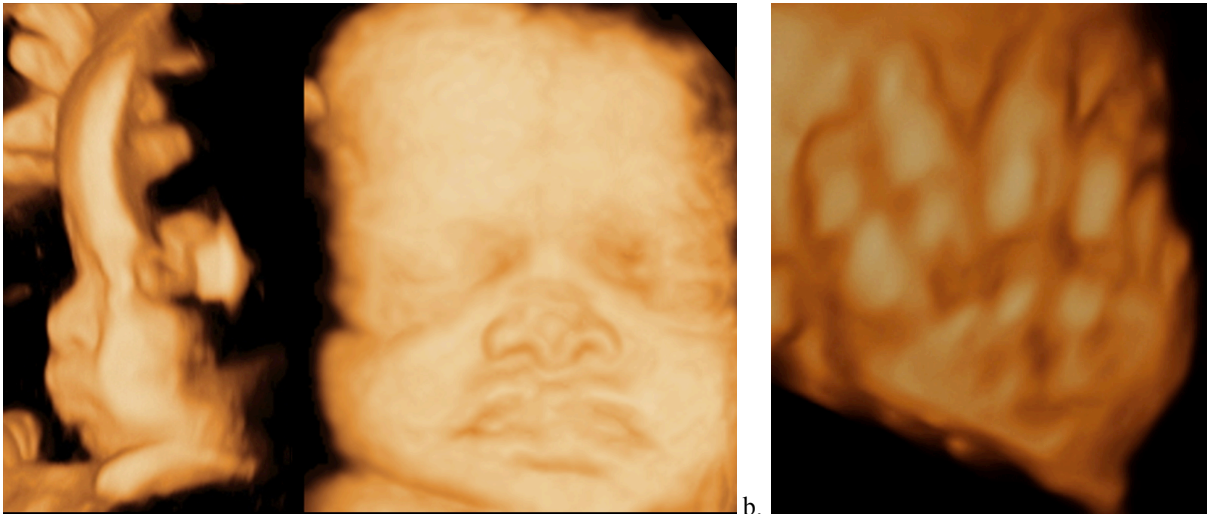


Figure S19 Surface rendered three-dimensional ultrasound imaging in a fetus with achondroplasia. (a) Fetal face at 29 weeks: profile (left) and frontal aspect (right). (b) Typical appearance of the fetal hand ('trident hand') at 31 weeks.

Osteogenesis imperfecta

Osteogenesis imperfecta (OI) belongs to Group 25 of the current classification⁵⁸, the OI and decreased bone density group, a large group of skeletal disorders with abnormally developed, fragile bones. The number of identified gene defects responsible for OI types is increasing. Multiple fractures are common and, in severe cases, can occur prenatally. In serious lethal OI types there may be abnormal bending of the calvarium. Typical signs are the compressible, translucent skull and, on rendered views, the brittle skull bones (Figure 8).

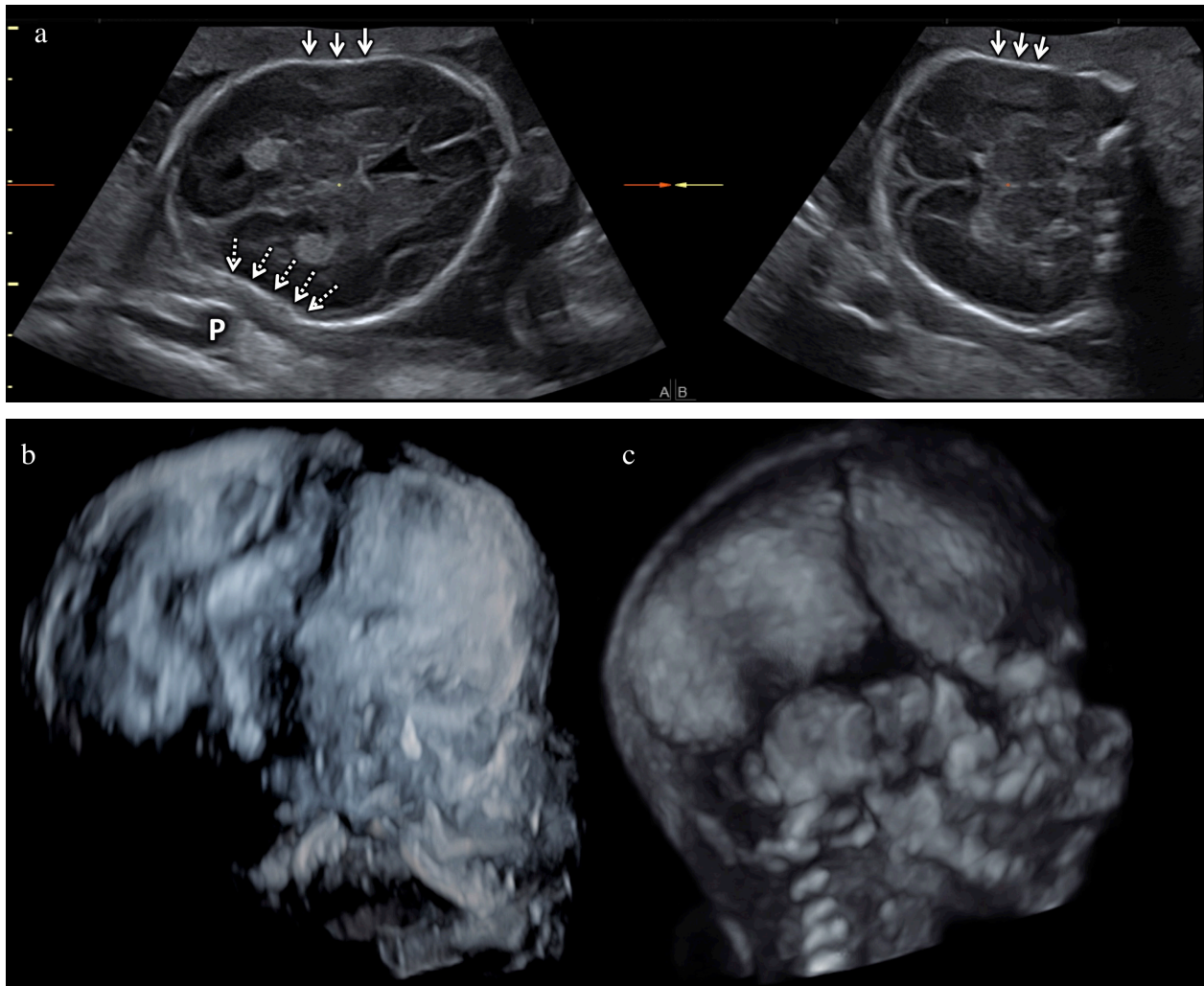


Figure 8 Three-dimensional ultrasound of the skull of a 22-week fetus with osteogenesis imperfecta. (a) On cross-sectional imaging the skull is less echogenic and more compressible than normal; compression of the membranaceous skull by pressure from the transducer (solid arrows) and the maternal promontorium (P; dotted arrows). (b) Surface reconstruction of the skull shows the less echogenic, irregular and brittle appearance of the calvarian bones. (c) Age-matched normal fetal skull.

Craniosynostosis

Pretorius and Nelson first demonstrated the application of 3D-US for visualizing normal cranial sutures and fontanels⁴. Many other 3D-US studies have described various features of the fetal cranium, both normal and abnormal^{5,6,62-66}. Any decision to use 3D-US for bone imaging should be based on its potential diagnostic value, and some investigators have reported improved characterization of fetal bone disorders⁶⁷⁻⁷⁰.

Osteochondrodysplasias are developmental disorders that may affect multiple fetal bones. In the current classification⁵⁸, Group 33, craniosynostosis syndromes, are skeletal disorders affecting the skull and face that may be amenable to 3D-US diagnosis.

Craniosynostoses are a heterogeneous group of anomalies with a prevalence of 1 in 2000, characterized by skull deformities often associated with premature closure of the cranial sutures⁷¹. This leads to characteristically deformed head shapes (Figure S20), depending on which particular sutures are involved, as a result of compensatory growth of the skull. Prenatally

diagnosed craniosynostoses include sagittal synostosis: scaphocephaly or dolichocephaly (long, slim head); coronal synostosis: brachycephaly (short head; Figure S21); and metopic synostosis: trigonocephaly (Figure S22). Asymmetrical closure of one coronal or lambdoid suture causes asymmetrical flattening of the head (plagiocephaly; Figure S20). Cloverleaf skull ('Kleeblattschädel') and oxycephaly (brachyturriccephaly; 'Turmschädel') result from various combinations of closure of coronal, lambdoid, squamous and sagittal sutures^{71,72}. Characteristic shapes of the craniosynostotic head in combination with other anatomical features may also indicate specific types (Table S1).

3D-US has been used successfully in fetuses with suspected skeletal dysplasia by analysis of facial dysmorphism, fingers and ossification status in osteochondrodysplasia^{67,73}. For example, brachycephaly in combination with a non-visualized cranial suture at the lateral axial position and mitten hands should raise the suspicion of craniosynostosis as part of Apert syndrome (Figure S21).

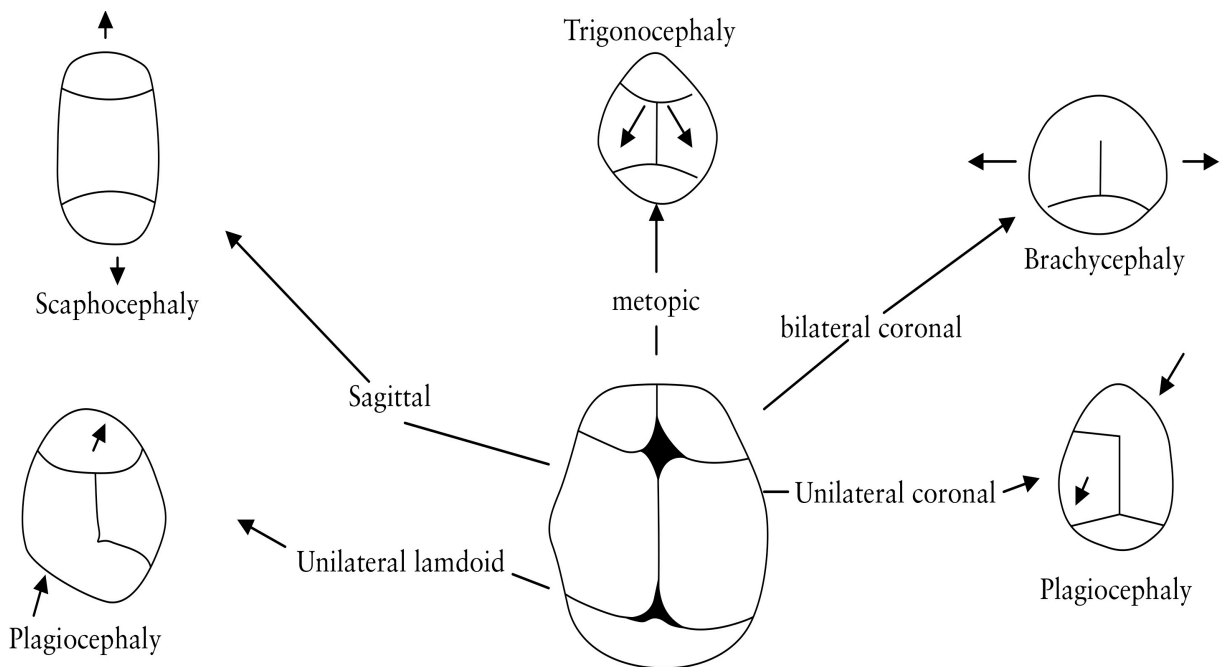


Figure S20 Schematic representation of head shapes in the presence of premature symmetrical or asymmetrical closure of cranial sutures (reproduced from Delahaye *et al.*⁷¹ with permission)

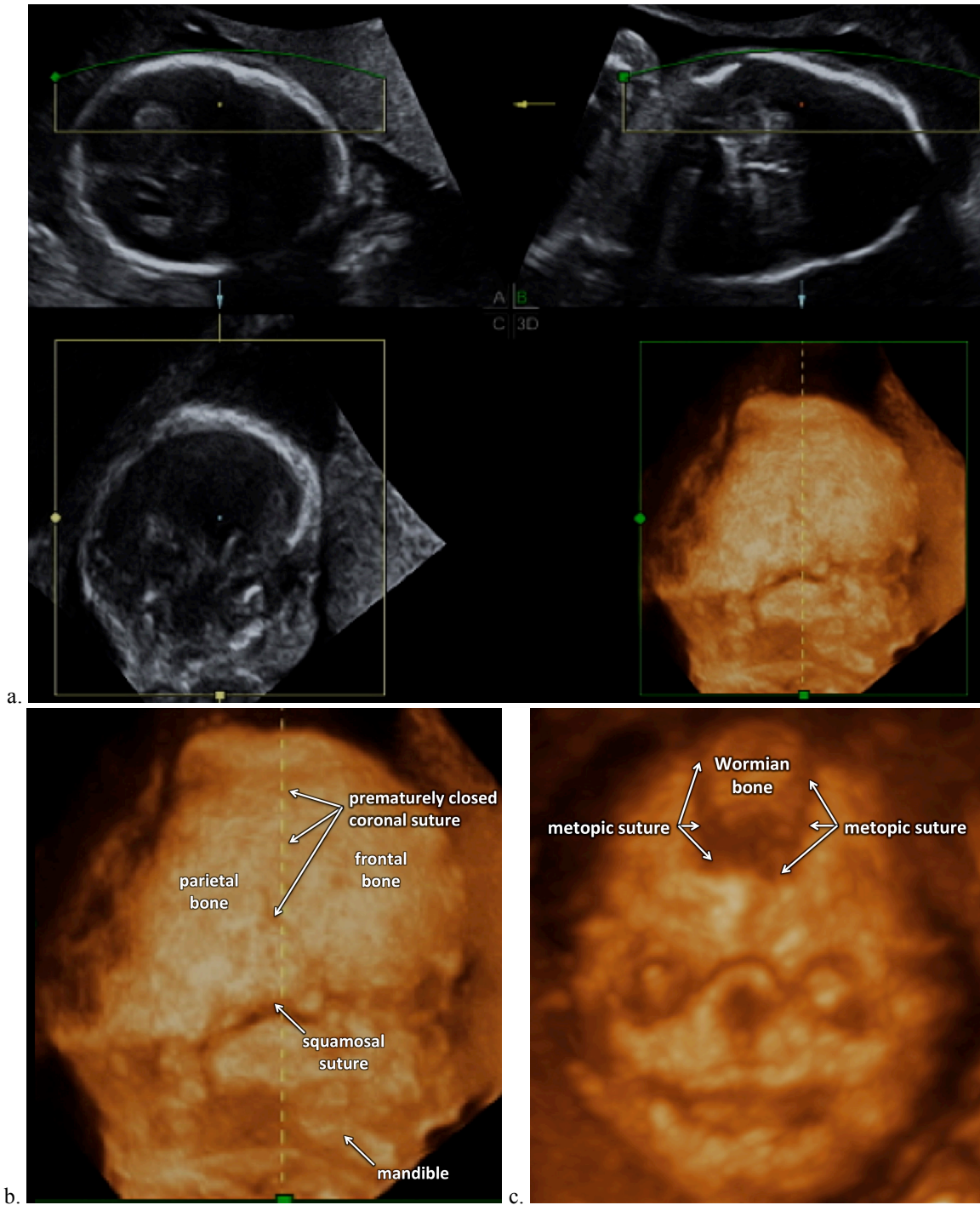


Figure S21 Craniosynostosis in Apert syndrome. (a) In this multiplanar display, panels A and B show brachytrurricephaly (short, high head). (b) Lateral aspect of fetal skull with apparent premature closure of coronal sutures (compare with normal skull in Figure 3). (c) Abnormally wide metopic suture with an intrasutural bone ('Wormian bone').



Figure S22 Surface rendering of fetal face following premature closure of metopic suture, resulting in trigonocephaly (pointed forehead with ridge; triangular head shape in axial views)

Table S1 Affected cranial sutures, skull deformities and associated anomalies in selected craniosynostoses (modified from Delahaye *et al.*⁷¹, Keating⁷² and GeneReviews (<http://www.ncbi.nlm.nih.gov/books/NBK1189/>)). Pfeiffer syndrome (fibroblast growth factor receptor 1 (FGFR1) and FGFR2-related), Apert syndrome (FGFR2-related) and Crouzon syndrome (FGFR2-related) belong to Group 33, the craniosynostosis group, which includes 15 different conditions⁵⁸

Syndrome	Affected sutures	Skull and head	Associated anomalies, additional information
Apert	Coronal, sagittal, lambdoid	Turricephaly ('Turmschädel'; short, high skull), midface hypoplasia, hypertelorism, marked nasal bridge	Syndactyly (symmetrical, hands and feet), 'mitten-like' hand, impaired vision and hearing, broad thumb, broad great toe, impaired neurodevelopment possible
Pfeiffer	Coronal, sagittal	Brachycephaly, some have cloverleaf skull ('Kleeblattschädel'; in Pfeiffer type 2), protruding eye balls	Polysyndactyly, abducted thumb, no impaired neurodevelopment
Crouzon	Coronal, sagittal	Turricephaly, exophthalmia, hypertelorism, maxillary retrognathia, mandibular prognathism	Usually no impaired neurodevelopment; seldom syndactyly

Other conditions with abnormal sutures and fontanels

Using 3D-US, the metopic suture and the anterior fontanel have also been shown to be abnormal in several other pathological conditions. Malformative and genetic syndromes as well as aneuploidies may exhibit premature closure, abnormal shape or widening of the metopic suture^{6,62-65}. The anterior fontanel is enlarged in mid-trimester fetuses with trisomy 21⁷⁴. Examples of normal and abnormal metopic sutures and anterior fontanels are shown in Figure S23.

Other skeletal dysplasias with abnormal profile

An abnormal profile occurs in a large number of genetic disorders. Group 34, dysostoses with predominant craniofacial involvement⁵⁸, includes at least 13 different disorders, such as Goldenhar syndrome (hemifacial microsomia), Treacher–Collins syndrome (mandibula-facial dysostosis; sonographic features include micrognathia and missing or malformed external ears) and frontonasal dysplasia (hypertelorism and broad nose due to various degrees of median clefting), that are rare but well-known conditions. Case reports have described the diagnosis of such facial anomalies using 2D-US and illustrated how the use of 3D-US helped to better define the final diagnosis⁷⁵⁻⁷⁷.

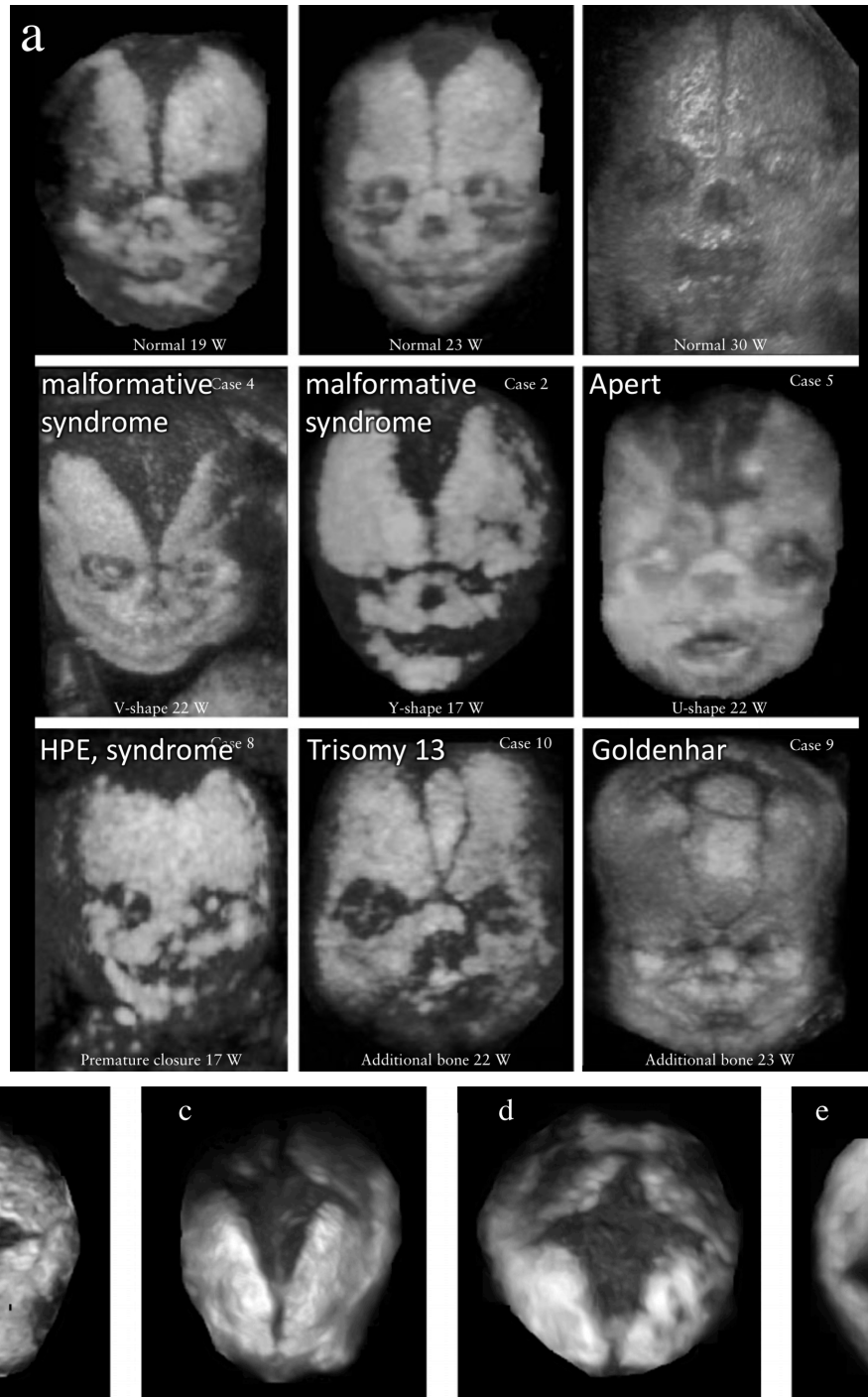


Figure S23 Normal and abnormal metopic suture (a) and anterior fontanel (b–e). (a) Normal metopic sutures at 19, 23 and 30 gestational weeks (top row) and metopic sutures in malformative, genetic or chromosomal syndromes between 17 and 23 weeks (middle and bottom rows; reproduced from Chaoui *et al.*⁶ with permission). (b) Normal anterior fontanel at 20 weeks. (c,d,e) Anterior fontanel in Down-syndrome fetuses at 21, 20 and 22 weeks, respectively (reproduced from Paladini *et al.*⁷⁴ with permission). HPE, holoprosencephaly.

Summary

Since the first report by Pretorius and Nelson⁴ demonstrating the application of 3D-US for visualizing normal cranial sutures and fontanelles, a number of 3D-US studies have been published describing the normal and abnormal fetal cranium as well as normal and abnormal development of the fetal skull, facial bones and palate^{5-7,62,66}. 3D-US is complementary to 2D-US, but more accurate in demonstrating subtle facial features and for measuring distances, angles and sizes in defined anatomical planes. Several authors suggest that 3D-US improves the accuracy of prenatal diagnosis of skeletal disorders^{67-70,73}.

Different 3D-US display modalities can be used to visualize the fetal skeleton. Cross-sectional modes allow a detailed anatomical study of all osseous and soft tissues; these can be of invaluable help in the differential diagnosis of skull anomalies. The rendered views can provide high levels of detail, of the curved skull bones; however, they are prone to specific artifacts, as described above.

For the fetal skull, as for other fetal organs and body parts, 3D-US is not considered a primary screening tool, but in fetuses with skull anomalies suspected or diagnosed using real-time B-mode imaging, the additional use of 3D-US may clarify details not recognized in the initial 2D examination. It would be a misunderstanding and an oversimplification to assume that an US volume that physically contains the structures of interest can simply be acquired and processed to show the desired bony structures, as is possible with fetal computed tomography⁷⁸. Successful application of 3D-US, particularly for imaging of the skull, mandates prior knowledge of both the anatomical structures and their pathologies to optimize volume acquisition for these features. The appearance of the skull bones depends to a large extent on the insonation angle, i.e. the initial plane of volume acquisition, as has been shown previously for intracranial structures⁷⁹.

Specific areas that benefit from 3D-US include assessment of the abnormal fetal profile, craniosynostoses and facial clefts, all of which may be associated with chromosomal or genetic syndromes.

REFERENCES

1. Pilu G, Reece EA, Romero R, Bovicelli L, Hobbins JC. Prenatal diagnosis of craniofacial malformations with ultrasonography. *Am J Obstet Gynecol* 1986; **155**: 45–50.
2. Salomon LJ, Alfrevic Z, Berghella V, Bilardo C, Hernandez-Andrade E, Johnsen SL, Kalache K, Leung KY, Malinger G, Munoz H, Prefumo F, Toi A, Lee W, Committee ICS. Practice guidelines for performance of the routine mid-trimester fetal ultrasound scan. *Ultrasound Obstet Gynecol* 2011; **37**: 116–126.
3. Merz E, Abramovicz J, Baba K, Blaas HG, Deng J, Gindes L, Lee W, Platt L, Pretorius D, Schild R, Sladkevicius P, Timor-Tritsch I. 3D imaging of the fetal face - recommendations from the International 3D Focus Group. *Ultraschall Med* 2012; **33**: 175–182.
4. Pretorius DH, Nelson TR. Prenatal visualization of cranial sutures and fontanelles with three-dimensional ultrasonography. *J Ultrasound Med* 1994; **13**: 871–876.
5. Dikkeboom CM, Roelfsema NM, Van Adrichem LN, Wladimiroff JW. The role of three-dimensional ultrasound in visualizing the fetal cranial sutures and fontanelles during the second half of pregnancy. *Ultrasound Obstet Gynecol* 2004; **24**: 412–416.
6. Chaoui R, Levailant JM, Benoit B, Faro C, Wegrzyn P, Nicolaides KH. Three-dimensional sonographic description of abnormal metopic suture in second- and third-trimester fetuses. *Ultrasound Obstet Gynecol* 2005; **26**: 761–764.
7. Faro C, Benoit B, Wegrzyn P, Chaoui R, Nicolaides KH. Three-dimensional sonographic description of the fetal frontal bones and metopic suture. *Ultrasound Obstet Gynecol* 2005; **26**: 618–621.
8. Ashhurst DE. Assessing skeletal development. *Ultrasound Obstet Gynecol* 1997; **9**: 373.
9. Achiron R, Gindes L, Zalel Y, Lipitz S, Weisz B. Three- and four-dimensional ultrasound: new methods for evaluating fetal thoracic anomalies. *Ultrasound Obstet Gynecol* 2008; **32**: 36–43.
10. Benacerraf BR, Benson CB, Abuhamad AZ, Copel JA, Abramowicz JS, Devore GR, Doubilet PM, Lee W, Lev-Toaff AS, Merz E, Nelson TR, O'Neill MJ, Parsons AK, Platt LD, Pretorius DH, Timor-Tritsch IE. Three- and 4-dimensional ultrasound in obstetrics and gynecology: proceedings of the American Institute of Ultrasound in Medicine Consensus Conference. *J Ultrasound Med* 2005; **24**: 1587–1597.
11. Benacerraf BR, Shipp TD, Bromley B. How sonographic tomography will change the face of obstetric sonography: a pilot study. *J Ultrasound Med* 2005; **24**: 371–378.
12. Espinoza J, Romero R, Kusanovic JP, Gotsch F, Lee W, Goncalves LF, Hassan SS. Standardized views of the fetal heart using four-dimensional sonographic and tomographic imaging. *Ultrasound Obstet Gynecol* 2008; **31**: 233–242.
13. Merz E, Benoit B, Blaas HG, Baba K, Kratochwil A, Nelson T, Pretorius D, Jurkovic D, Chang FM, Lee A, Group IDF. Standardization of three-dimensional images in obstetrics and gynecology: consensus statement. *Ultrasound Obstet Gynecol* 2007; **29**: 697–703.
14. Jones KL. *Smith's Recognizable Patterns of Human Malformations*. W.B. Saunders: Philadelphia, 1997.
15. de Jong-Pleij EA, Ribbert LS, Manten GT, Tromp E, Bilardo CM. Maxilla-nasion-mandible angle: a new method to assess profile anomalies in pregnancy. *Ultrasound Obstet Gynecol* 2011; **37**: 562–569.
16. Rotten D, Levailant JM. Two- and three-dimensional sonographic assessment of the fetal face. 1. A systematic analysis of the normal face. *Ultrasound Obstet Gynecol* 2004; **23**: 224–231.
17. Rotten D, Levailant JM, Martinez H, Ducou le Pointe H, Vicaut E. The fetal mandible: a 2D and 3D sonographic approach to the diagnosis of retrognathia and micrognathia. *Ultrasound Obstet Gynecol* 2002; **19**: 122–130.
18. Rotten D, Levailant JM. Two- and three-dimensional sonographic assessment of the fetal face. 2. Analysis of cleft lip, alveolus and palate. *Ultrasound Obstet Gynecol* 2004; **24**: 402–411.

19. De Jong-Pleij EA, Ribbert LS, Tromp E, Bilardo CM. Three-dimensional multiplanar ultrasound is a valuable tool in the study of the fetal profile in the second trimester of pregnancy. *Ultrasound Obstet Gynecol* 2010; **35**: 195–200.
20. Merz E, Weber G, Bahlmann F, Miric-Tesanic D. Application of transvaginal and abdominal three-dimensional ultrasound for the detection or exclusion of malformations of the fetal face. *Ultrasound Obstet Gynecol* 1997; **9**: 237–243.
21. Vos FI, de Jong-Pleij EA, Bakker M, Tromp E, Kagan KO, Bilardo CM. Fetal facial profile markers of Down syndrome in the second and third trimesters of pregnancy. *Ultrasound Obstet Gynecol* 2015; **46**: 168–173.
22. de Jong-Pleij EA, Ribbert LS, Pistorius LR, Tromp E, Bilardo CM. The fetal profile line: a proposal for a sonographic reference line to classify forehead and mandible anomalies in the second and third trimester. *Prenat Diagn* 2012; **32**: 797–802.
23. Faure JM, Baumler M, Boulot P, Bigorre M, Captier G. Prenatal assessment of the normal fetal soft palate by three-dimensional ultrasound examination: is there an objective technique? *Ultrasound Obstet Gynecol* 2008; **31**: 652–656.
24. Wilhelm L, Braumann B. [Sonographic evaluation of fetal clefts of the lip, alveolus and palate]. *Z Geburtshilfe Neonatol* 2012; **216**: 63–72.
25. Benoit B, Chaoui R. Three-dimensional ultrasound with maximal mode rendering: a novel technique for the diagnosis of bilateral or unilateral absence or hypoplasia of nasal bones in second-trimester screening for Down syndrome. *Ultrasound Obstet Gynecol* 2005; **25**: 19–24.
26. Merz E, Abramowicz JS. 3D/4D ultrasound in prenatal diagnosis: is it time for routine use? *Clin Obstet Gynecol* 2012; **55**: 336–351.
27. Roelfsema NM, Grijseels EW, Hop WC, Wladimiroff JW. Three-dimensional sonography of prenatal skull base development. *Ultrasound Obstet Gynecol* 2007; **29**: 372–377.
28. Roelfsema NM, Hop WC, van Adrichem LN, Wladimiroff JW. Craniofacial variability index in utero: a three-dimensional ultrasound study. *Ultrasound Obstet Gynecol* 2007; **29**: 258–264.
29. Levailant JM, Mabilille M. Fetal sphenoid bone: imaging using three-dimensional ultrasound and computed tomography. *Ultrasound Obstet Gynecol* 2008; **31**: 229–231.
30. Degani S, Leibovitz Z, Shapiro I, Gonen R, Ohel G. Ultrasound evaluation of the fetal skull base throughout pregnancy. *Ultrasound Obstet Gynecol* 2002; **19**: 461–466.
31. Leibovitz Z, Egenburg S, Bronshtein M, Shapiro I, Tepper R, Malinger G, Ohel G. Sonographic imaging of fetal tympanic rings. *Ultrasound Obstet Gynecol* 2013; **42**: 536–544.
32. Nelson TR, Pretorius DH, Hull A, Riccabona M, Sklansky MS, James G. Sources and impact of artifacts on clinical three-dimensional ultrasound imaging. *Ultrasound Obstet Gynecol* 2000; **16**: 374–383.
33. Pretorius DH, House M, Nelson TR, Hollenbach KA. Evaluation of normal and abnormal lips in fetuses: comparison between three- and two-dimensional sonography. *AJR Am J Roentgenol* 1995; **165**: 1233–1237.
34. Dyson RL, Pretorius DH, Budorick NE, Johnson DD, Sklansky MS, Cantrell CJ, Lai S, Nelson TR. Three-dimensional ultrasound in the evaluation of fetal anomalies. *Ultrasound Obstet Gynecol* 2000; **16**: 321–328.
35. Merz E, Welter C. 2D and 3D Ultrasound in the evaluation of normal and abnormal fetal anatomy in the second and third trimesters in a level III center. *Ultraschall Med* 2005; **26**: 9–16.
36. Paladini D, Morra T, Teodoro A, Lamberti A, Tremolaterra F, Martinelli P. Objective diagnosis of micrognathia in the fetus: the jaw index. *Obstet Gynecol* 1999; **93**: 382–386.
37. Roelfsema NM, Hop WC, Wladimiroff JW. Three-dimensional sonographic determination of normal fetal mandibular and maxillary size during the second half of pregnancy. *Ultrasound Obstet Gynecol* 2006; **28**: 950–957.

38. Paladini D. Fetal micrognathia: almost always an ominous finding. *Ultrasound Obstet Gynecol* 2010; **35**: 377–384.
39. Cicero S, Bindra R, Rembouskos G, Tripsanas C, Nicolaides KH. Fetal nasal bone length in chromosomally normal and abnormal fetuses at 11–14 weeks of gestation. *J Matern Fetal Neonatal Med* 2002; **11**: 400–402.
40. Cicero S, Curcio P, Papageorghiou A, Sonek J, Nicolaides K. Absence of nasal bone in fetuses with trisomy 21 at 11–14 weeks of gestation: an observational study. *Lancet* 2001; **358**: 1665–1667.
41. Cicero S, Sonek JD, McKenna DS, Croom CS, Johnson L, Nicolaides KH. Nasal bone hypoplasia in trisomy 21 at 15–22 weeks' gestation. *Ultrasound Obstet Gynecol* 2003; **21**: 15–18.
42. Rembouskos G, Cicero S, Longo D, Vandecruys H, Nicolaides KH. Assessment of the fetal nasal bone at 11–14 weeks of gestation by three-dimensional ultrasound. *Ultrasound Obstet Gynecol* 2004; **23**: 232–236.
43. Minderer S, Gloning KP, Henrich W, Stoger H. The nasal bone in fetuses with trisomy 21: sonographic versus pathomorphological findings. *Ultrasound Obstet Gynecol* 2003; **22**: 16–21.
44. Jensen BL, Kreiborg S, Dahl E, Fogh-Andersen P. Cleft lip and palate in Denmark, 1976–1981: epidemiology, variability, and early somatic development. *Cleft Palate J* 1988; **25**: 258–269.
45. Johnson DD, Pretorius DH, Budorick NE, Jones MC, Lou KV, James GM, Nelson TR. Fetal lip and primary palate: three-dimensional versus two-dimensional US. *Radiology* 2000; **217**: 236–239.
46. Lee W, McNie B, Chaiworapongsa T, Conoscenti G, Kalache KD, Vettraino IM, Romero R, Comstock CH. Three-dimensional ultrasonographic presentation of micrognathia. *J Ultrasound Med* 2002; **21**: 775–781.
47. Campbell S, Lees CC. The three-dimensional reverse face (3D RF) view for the diagnosis of cleft palate. *Ultrasound Obstet Gynecol* 2003; **22**: 552–554.
48. Benacerraf BR, Sadow PM, Barnewolt CE, Estroff JA, Benson C. Cleft of the secondary palate without cleft lip diagnosed with three-dimensional ultrasound and magnetic resonance imaging in a fetus with Fryns' syndrome. *Ultrasound Obstet Gynecol* 2006; **27**: 566–570.
49. Baumler M, Faure JM, Bigorre M, Baumler-Patris C, Boulot P, Demattei C, Captier G. Accuracy of prenatal three-dimensional ultrasound in the diagnosis of cleft hard palate when cleft lip is present. *Ultrasound Obstet Gynecol* 2011; **38**: 440–444.
50. Offerdal K, Jebens N, Syvertsen T, Blaas HG, Johansen OJ, Eik-Nes SH. Prenatal ultrasound detection of facial clefts: a prospective study of 49,314 deliveries in a non-selected population in Norway. *Ultrasound Obstet Gynecol* 2008; **31**: 639–646.
51. Faure JM, Baumler M, Bigorre M, Captier G, Boulot P. Prenatal diagnosis of an isolated incomplete V-shaped cleft palate using a new three-dimensional ultrasound technique investigation. *Surg Radiol Anat* 2007; **29**: 695–698.
52. Platt LD, Devore GR, Pretorius DH. Improving cleft palate/cleft lip antenatal diagnosis by 3-dimensional sonography: the "flipped face" view. *J Ultrasound Med* 2006; **25**: 1423–1430.
53. Levailant JM, Nicot R, Benouaiche L, Couly G, Rotten D. Prenatal diagnosis of cleft lip/palate: The surface rendered oro-palatal (SROP) view of the fetal lips and palate, a tool to improve information-sharing within the orofacial team and with the parents. *J Craniomaxillofac Surg* 2016; **44**: 835–842.
54. Merz E, Pashaj S. [Prenatal detection of orofacial clefts]. *Ultraschall Med* 2016; **37**: 133–135.

55. Pilu G, Segata M. A novel technique for visualization of the normal and cleft fetal secondary palate: angled insonation and three-dimensional ultrasound. *Ultrasound Obstet Gynecol* 2007; **29**: 166–169.
56. Martinez Ten P, Perez Pedregosa J, Santacruz B, Adiego B, Barron E, Sepulveda W. Three-dimensional ultrasound diagnosis of cleft palate: 'reverse face', 'flipped face' or 'oblique face'--which method is best? *Ultrasound Obstet Gynecol* 2009; **33**: 399–406.
57. Rotten D, Levailant JM, Benouaiche L, Nicot R, Couly G. Visualization of fetal lips and palate using a surface-rendered oropalatal (SROP) view in fetuses with normal palate or orofacial cleft lip with or without cleft palate. *Ultrasound Obstet Gynecol* 2016; **47**: 244–246.
58. Bonafe L, Cormier-Daire V, Hall C, Lachman R, Mortier G, Mundlos S, Nishimura G, Sangiorgi L, Savarirayan R, Sillence D, Spranger J, Superti-Furga A, Warman M, Unger S. Nosology and classification of genetic skeletal disorders: 2015 revision. *Am J Med Genet A* 2015; **167A**: 2869–2892.
59. Schramm T, Gloning KP, Minderer S, Daumer-Haas C, Hortnagel K, Nerlich A, Tutschek B. Prenatal sonographic diagnosis of skeletal dysplasias. *Ultrasound Obstet Gynecol* 2009; **34**: 160–170.
60. Blaas HG, Vogt C, Eik-Nes SH. Abnormal gyration of the temporal lobe and megalencephaly are typical features of thanatophoric dysplasia and can be visualized prenatally by ultrasound. *Ultrasound Obstet Gynecol* 2012; **40**: 230–234.
61. Shirley ED, Ain MC. Achondroplasia: manifestations and treatment. *J Am Acad Orthop Surg* 2009; **17**: 231–241.
62. Paladini D, Vassallo M, Sglavo G, Pastore G, Lapadula C, Nappi C. Normal and abnormal development of the fetal anterior fontanelle: a three-dimensional ultrasound study. *Ultrasound Obstet Gynecol* 2008; **32**: 755–761.
63. Faro C, Chaoui R, Wegrzyn P, Levailant JM, Benoit B, Nicolaidis KH. Metopic suture in fetuses with Apert syndrome at 22–27 weeks of gestation. *Ultrasound Obstet Gynecol* 2006; **27**: 28–33.
64. Faro C, Wegrzyn P, Benoit B, Chaoui R, Nicolaidis KH. Metopic suture in fetuses with trisomy 21 at 11 + 0 to 13 + 6 weeks of gestation. *Ultrasound Obstet Gynecol* 2006; **27**: 286–289.
65. Faro C, Wegrzyn P, Benoit B, Chaoui R, Nicolaidis KH. Metopic suture in fetuses with holoprosencephaly at 11 + 0 to 13 + 6 weeks of gestation. *Ultrasound Obstet Gynecol* 2006; **27**: 162–166.
66. David AL, Turnbull C, Scott R, Freeman J, Bilardo CM, van Maarle M, Chitty LS. Diagnosis of Apert syndrome in the second-trimester using 2D and 3D ultrasound. *Prenat Diagn* 2007; **27**: 629–632.
67. Ruano R, Molho M, Roume J, Ville Y. Prenatal diagnosis of fetal skeletal dysplasias by combining two-dimensional and three-dimensional ultrasound and intrauterine three-dimensional helical computer tomography. *Ultrasound Obstet Gynecol* 2004; **24**: 134–140.
68. Tsai PY, Chang CH, Yu CH, Cheng YC, Chang FM. Thanatophoric dysplasia: role of 3-dimensional sonography. *J Clin Ultrasound* 2009; **37**: 31–34.
69. Kennelly MM, Moran P. A clinical algorithm of prenatal diagnosis of Radial Ray Defects with two and three dimensional ultrasound. *Prenat Diagn* 2007; **27**: 730–737.
70. Garjian KV, Pretorius DH, Budorick NE, Cantrell CJ, Johnson DD, Nelson TR. Fetal skeletal dysplasia: three-dimensional US--initial experience. *Radiology* 2000; **214**: 717–723.
71. Delahaye S, Bernard JP, Renier D, Ville Y. Prenatal ultrasound diagnosis of fetal craniosynostosis. *Ultrasound Obstet Gynecol* 2003; **21**: 347–353.
72. Keating RF. Craniosynostosis: diagnosis and management in the new millennium. *Pediatr Ann* 1997; **26**: 600–612.

73. Krakow D, Williams J, 3rd, Poehl M, Rimoin DL, Platt LD. Use of three-dimensional ultrasound imaging in the diagnosis of prenatal-onset skeletal dysplasias. *Ultrasound Obstet Gynecol* 2003; **21**: 467–472.
74. Paladini D, Sglavo G, Penner I, Pastore G, Nappi C. Fetuses with Down syndrome have an enlarged anterior fontanelle in the second trimester of pregnancy. *Ultrasound Obstet Gynecol* 2007; **30**: 824–829.
75. Johnstone E, Glanville T, Pilling J, Dobbie A. Prenatal diagnosis of frontonasal dysplasia using 3D ultrasound. *Prenat Diagn* 2008; **28**: 1075–1076.
76. Guzelmansur I, Ceylaner G, Ceylaner S, Ceylan N, Daplan T. Prenatal diagnosis of Goldenhar syndrome with unusual features by 3D ultrasonography. *Genet Couns* 2013; **24**: 319–325.
- <EPATH>77. Treacher Collins syndrome – role of 3D/4D ultrasound in the assessment of fetal facial dysmorphism. <https://sonoworld.com/TheFetus/page.aspx?id=3491>.
78. Cassart M, Massez A, Cos T, Tecco L, Thomas D, Van Regemorter N, Avni F. Contribution of three-dimensional computed tomography in the assessment of fetal skeletal dysplasia. *Ultrasound Obstet Gynecol* 2007; **29**: 537–543.
79. Plasencia W, Dagklis T, Borenstein M, Csapo B, Nicolaides KH. Assessment of the corpus callosum at 20–24 weeks' gestation by three-dimensional ultrasound examination. *Ultrasound Obstet Gynecol* 2007; **30**: 169–172.